NASA CONTRACTOR REPORT

NASA CR-1376

ASYMMETRIC NONLINEAR DYNAMIC RESPONSE AND BUCKLING OF SHALLOW SPHERICAL SHELLS

by Atis A. Liepins

Prepared by
DYNATECH CORPORATION
Cambridge, Mass.
for Langley Research Center

NATIONAL AERONAUTICS AND SPACE ADMINISTRATION • WASHINGTON, D. C. • JUNE 1969

NASA CR-1376

ASYMMETRIC NONLINEAR DYNAMIC RESPONSE AND BUCKLING OF SHALLOW SPHERICAL SHELLS

By Atis A. Liepins

Prepared under Contract No. NAS 1-6586 by
DYNATECH CORPORATION
Cambridge, Mass.

for Langley Research Center

NATIONAL AERONAUTICS AND SPACE ADMINISTRATION

For sale by the Clearinghouse for Federal Scientific and Technical Information
Springfield, Virginia 22151 – CFSTI price $3.00

CONTENTS

ILLUSTRATIONS

Figure

ASYMMETRIC NONLINEAR DYNAMIC RESPONSE AND BUCKLING OF SHALLOW SPHERICAL SHELLS

by Atis A. Liepins
Dynatech Corporation

SUMMARY

A numerical method and computer program are developed for the computation of the large deflection dynamic response of simply supported shallow spherical shells subjected to a class of spatially asymmetric and timewise step loadings. The numerical method employs two dimensional spatial finite differences, timewise finite differences together with Houbolt's method, and solution by Newton's procedure together with an extension of Potters method. Response histories and asymmetric dynamic buckling loads for several geometries and load durations are presented.

INTRODUCTION

Thin shell components have found wide application in spacecraft structures. For example, the Apollo command module aft heat shield back-up structure is a thin spherical shell. The behavior of shell structures under impact loads is of importance in the design of such structures to withstand water landing loads. Of special interest is the response and instability of thin spherical shells subjected to time dependent spatially asymmetric loadings.

The literature on the numerical calculation of large deflection dynamic response and instability of thin shallow spherical shells is sparse. A recent review of the literature can be found in Reference 1. All studies reviewed in Reference 1 are limited to symmetric response. To the author's knowledge, reports on the asymmetric nonlinear dynamic response of shells have not appeared in the literature.

The purpose of the present analysis is to develop a numerical method and computer program for the calculation of the large deflection dynamic response of simply supported shallow spherical shells subjected to a class of spatially asymmetric and timewise step loadings. The program is then used to calculate asymmetric dynamic buckling loads for a few geometries and load durations.

NOMENCLATURE

a	base radius of shell
h	thickness of shell
p	nondimensional pressure
q	pressure
q_0	classical buckling pressure for complete sphere
r	radial coordinate
t	time
w	nondimensional normal displacement
x	nondimensional radial coordinate
D	$Eh^3/12\,(1 - \nu^2)$
E	Young's modulus
F	stress function
H	initial height of shell at the pole
$H(\tau)$	unit step function
I_{cr}	critical impulse
M	number of finite difference stations on a meridian
$M_r, M_\theta, M_{r\theta}$	stress couples
N	number of meridians less one in the finite difference net
$N_r, N_\theta, N_{r\theta}$	stress resultants
R	radius of curvature
T	kinetic energy
U	meridional displacement

V	circumferential displacement
$\overline{V}$	volume of deformation
$\overline{V}_D$	volume difference
W	normal displacement

α	measure of asymmetry of load
ϵ	convergence tolerance
$\epsilon_r, \epsilon_\theta, \epsilon_{r\theta}$	membrane strains
ζ	location of middle surface above base plane
η	static load increment reduction factor
θ	circumferential coordinate
$\kappa_r, \kappa_\theta, \kappa_{r\theta}$	bending strains
λ	geometry parameter
ν	Poisson's ratio
ρ	material density
τ	nondimensional time
τ^*	duration of load
ψ	nondimensional stress function
Δx	meridional finite difference spacing
$\Delta \theta$	circumferential finite difference spacing
$\Delta \tau$	timewise finite difference spacing

Matrices

A_L	linear static coefficient matrix
A_{NL}	nonlinear static coefficient matrix
A_D	dynamic coefficient matrix
F_L	load column matrix
F_{NL}	pseudo load column matrix
F_D	dynamic column matrix
Z	column matrix of all mesh variables

Indices

k	time station
m	meridional station
n	circumferential station
r	iteration in Newton's procedure

GOVERNING EQUATIONS

The shell is assumed to be 1) thin, that is, the ratio of wall thickness to radius of curvature is much less than unity; 2) shallow, the ratio of the rise at the pole to the base diameter is less than about 1/8; 3) elastic; 4) undergoing small strains despite large deflections; and 5) imperfection free. The geometry of the shell and notation are shown in Figure 1.

The load is distributed over the surface of the shell asymmetrically, consisting of uniform and linearly varying parts, as shown in Figure 1. Timewise the load is applied suddenly, held with constant intensity for a finite duration of time, and removed suddenly.

The analysis is based upon the shallow shell equations of Marguerre [2]. In terms of nondimensional variables these are:

$$\nabla^4 w - \nabla^2 \psi = \left(\frac{1}{x}\psi' + \frac{1}{x^2}\ddot{\psi}\right) w'' + \left(\frac{1}{x} w' + \frac{1}{x^2}\ddot{w}\right) \psi''$$

$$- 2\left(\frac{1}{x}\dot{\psi}' - \frac{1}{x^2}\dot{\psi}\right)\left(\frac{1}{x}\dot{w}' - \frac{1}{x^2}\dot{w}\right) + 4pH(\tau)\left(1 - \alpha \frac{x}{\lambda}\cos\theta\right) - \overset{**}{w} \qquad (1)$$

$$-\nabla^2 w - \nabla^4 \psi = \left(\frac{1}{x} w' + \frac{1}{x^2}\ddot{w}\right) w'' - \left(\frac{1}{x}\dot{w}' - \frac{1}{x^2}\dot{w}\right)^2 \qquad (2)$$

where $$\nabla^2 = \frac{\partial^2}{\partial x^2} + \frac{1}{x}\frac{\partial}{\partial x} + \frac{1}{x^2}\frac{\partial^2}{\partial \theta^2} = ()'' + \frac{1}{x}()' + \frac{1}{x^2}\ddot{()}$$

$$\frac{\partial}{\partial \tau} = \overset{*}{()}$$

$$\lambda^4 = 48(1 - \nu^2)\left(\frac{H}{h}\right)^2$$

$$x = \frac{\lambda}{a} r$$

$$\tau = \left(\frac{E}{\rho R^2}\right)^{1/2} t$$

$$w = \frac{\lambda^2}{2H} W$$

$$\psi = \frac{\lambda^4}{4EH^2h} F$$

$$p = \frac{q}{q_0}$$

$$q_0 = \frac{32\, EH^3h}{\lambda^2 a^4}$$

q_0 is the classical buckling pressure for a complete sphere [3], and $H(\tau)$ is the unit step function of finite duration which vanishes for $\tau < 0, \tau > \tau^*$ and equals unity for $0 \leq \tau \leq \tau^*$.

The stress function - stress relations are

$$N_r = \frac{1}{r} F' + \frac{1}{r^2} \ddot{F}$$

$$N_\theta = F''$$

$$N_{r\theta} = -\left(\frac{1}{r} \dot{F}\right)' . \tag{3}$$

The stress - strain relations are

$$\epsilon_r = \frac{1}{Eh} (N_r - \nu N_\theta)$$

$$\epsilon_\theta = \frac{1}{Eh} (N_\theta - \nu N_r)$$

$$\epsilon_{r\theta} = \frac{2(1+\nu)}{Eh} N_{r\theta}$$

$$M_r = D(\kappa_r + \nu \kappa_\theta)$$

$$M_\theta = D(\kappa_\theta + \nu \kappa_r)$$

$$M_{r\theta} = (1 - \nu) D \kappa_{r\theta} . \tag{4}$$

The strain - displacement relations are

$$\epsilon_r = U' + \frac{r}{R} W' + \frac{1}{2}(W')^2$$

$$\epsilon_\theta = \frac{1}{r} U + \frac{1}{r} \dot{V} + \frac{1}{2} \left(\frac{1}{r} \dot{W}\right)^2$$

$$\epsilon_{r\theta} = \frac{1}{r} \dot{U} - \frac{1}{r} V + V' + \frac{1}{R} \dot{W} + \frac{1}{r} \dot{W} W'$$

$$\kappa_r = - W''$$

$$\kappa_\theta = - \frac{1}{r} W' - \frac{1}{r^2} \ddot{W}$$

$$\kappa_{r\theta} = - \left(\frac{1}{r} \dot{W}\right)' . \qquad (5)$$

In equations (3) - (5), prime denotes differentiation with respect to r.

At $\tau = 0$ the shell is at rest:

$$w = \overset{*}{w} = \psi = \overset{*}{\psi} = 0 \qquad 0 \leq x \leq \lambda \qquad (6)$$
$$0 \leq \theta \leq \pi .$$

The edge of the shell at $x = \lambda$ is simply supported:

$$W = 0 ; \quad w = 0$$

$$U = 0 ; \quad \lambda \psi'' - \nu \psi' - \frac{\nu}{\lambda} \ddot{\psi} = 0$$

$$V = 0 ; \quad \lambda \psi''' - (1 - \nu) \frac{1}{\lambda} \psi' + (2 + \nu) \frac{1}{\lambda} \ddot{\psi}' - \frac{3}{\lambda^2} \ddot{\psi} + \lambda w' + \frac{1}{2}(w')^2 = 0$$

$$M_r = 0 ; \quad \lambda w'' + \nu w' = 0. \qquad (7)$$

Since the structure and loading are symmetric about the diameter $\theta = 0, \pi$ and deformations with such symmetry are assumed, we consider only one half of the shell corresponding to $0 \leq \theta \leq \pi$. The conditions on the diameter of symmetry are:

$$\dot{w} = \dot{\psi} = \dddot{w} = \dddot{\psi} = 0. \tag{8}$$

At the pole the stress resultants and bending moments must remain finite, there must be no transverse shear, and $N_r = N_\theta$. These requirements are satisfied if

$$\ddot{w} = \ddot{\psi} = 0$$

$$(w + \ddot{w})' = (\psi + \ddot{\psi})' = 0$$

$$\ddot{w}'' = \ddot{\psi}'' = 0 \tag{9}$$

at the pole.

Since the governing equations (1), (2), the boundary conditions (7), (8) and the pole conditions (9) do not involve ψ but only its derivatives, ψ is not uniquely determined. In fact,

$$w_Z = 0$$

$$\psi_Z = C_1(\tau) + C_2(\tau) \times \cos\theta \tag{10}$$

satisfy (1), (2), (7), (8), (9) at all times and cause no stress. If the nonlinear terms in the governing equations (1), (2) and the boundary conditions (7) are neglected, then the stress function solution may be written as

$$\psi = \psi_0(x, \tau) + \psi_1(x, \tau)\cos\theta + C_1(\tau) + C_2(\tau) \times \cos\theta \ . \tag{11}$$

The two functions C_1, C_2 in (11) may be determined by specifying the stress function to be zero at two points on the shell

$$\psi(\lambda, 0, \tau) = \psi(\lambda, \pi, \tau) = 0 \ . \tag{12}$$

Therefore for this particular loading and linear deformation it can be shown that (12) implies

$$\psi(\lambda, \theta, \tau) = 0 \ . \tag{13}$$

It is assumed that the application of (13) to the nonlinear equations (1), (2) and boundary conditions (7) results in a negligibly small error.

DERIVATION AND SOLUTION OF FINITE DIFFERENCE EQUATIONS

The solution to (1) and (2) is obtained by finite differences in time and two dimensional finite differences in space. Since an implicit difference method is used to march out the solution in time, nonlinear simultaneous equations have to be solved at each time step. These equations are solved by successive linearizations using Newton's procedure [4]. The Newton procedure computes successive corrections to the starting solution until the desired accuracy is obtained. Then the procedure is repeated at subsequent time steps until the solution is marched out to the desired time. Thus the most frequent step is the computation of the corrections in Newton's iteration procedure. The basic iteration equation is derived below.

The replacement of the derivatives in (1) and (2) by finite difference approximations is a common procedure for deriving finite difference analogues of (1) and (2). For the linear version of (1) and (2) this procedure will not always lead to finite difference equations with a symmetric matrix of coefficients, although linear structural behavior entitles us to a symmetric matrix. Another way to obtain finite difference equations is to derive them from a minimum principle as was done in References 5, 6, and 7. In the present case the equilibrium equation (1) may be obtained from Hamilton's Principle and the compatibility equation (2) may be obtained from the Principle of Minimum Complementary Energy. However, the use of two minimum principles for the present purpose is awkward. Instead, we derive finite difference analogues of (1) and (2) from the conditions for the stationary value of a definite integral

$$\delta \overline{F} = \delta \int_0^{\tau} (T - I)\, d\tau = 0 \tag{14}$$

where T is the kinetic energy associated with the transverse displacement of the shell

$$T = \frac{1}{2} \int_0^{\pi} \int_0^{\lambda} \overset{*}{w}^2 x\, dx\, d\theta \tag{15}$$

and

$$I = \int_0^{\pi}\int_0^{\lambda}\left[\frac{1}{2}(\nabla^2 w)^2 - \frac{1}{2}(\nabla^2\psi)^2 + \psi' w' + \frac{1}{x^2}\dot{\psi}\dot{w} - 4p\,H(\tau)\left(1-\alpha\frac{x}{\lambda}\cos\theta\right)w\right] x\,dx\,d\theta$$

$$+\int_0^{\pi}\int_0^{\lambda}\psi\left\{\left[\left(\frac{1}{x}\dot{w}\right)'\right]^2 - w''\left(\frac{1}{x}w' + \frac{1}{x^2}\dot{\dot{w}}\right)\right\} x\,dx\,d\theta$$

$$-\frac{1}{2}\int_0^{\pi}\left\{(1-\nu)(w')^2 - (1+\nu)\left[(\psi')^2 - \underline{\frac{1}{x^2}(\dot{\psi})^2} - \underline{2\dot{\psi}\left(\frac{1}{x}\dot{\psi}\right)'}\right] - \underline{\psi(w')^2}\right\}_{x=\lambda} d\theta \cdot \quad (16)$$

Although the integral (14) lacks physical meaning, it provides the basis for an orderly derivation of the finite difference analogues of (1) and (2).

Condition (14) is satisfied if w and ψ are solutions of the following differential equations,

$$\frac{d}{d\tau}\left(\frac{\partial T}{\partial \dot{Z}_i^*}\right) + \frac{\partial I}{\partial Z_i} = 0 \qquad i = 1,2 \qquad (17)$$

where $Z_1 = w$, and $Z_2 = \psi$. Equation (17) implies the governing equations (1) and (2), the boundary conditions (7) (8) and the pole conditions (9). If condition (13) is imposed, the underlined terms in (16) drop out, the conditions for the relative extremum of (14) are still such that equations (1), (2), (7), (8), (9) must be satisfied, and in addition ψ is determined uniquely. Thus the determination of the relative extremum of $\overline{F}$ without the underlined terms in (16) implies the solution of (1) and (2) subject to (6) - (9).

For the approximation of the integrals T and I we impose on the surface of the shell a net consisting of M parallels and N+1 meridians equally spaced such that

$$\Delta x = \frac{\lambda}{\left(M + \frac{1}{2}\right)}$$

$$\Delta\theta = \pi/N$$

$$x_m = m\Delta x \qquad m = 0,1,2,\ldots M$$

$$\theta_n = n\Delta\theta \qquad n = 0,1,2,\ldots N \qquad (18)$$

The edge of the shell appears halfway between two parallels.

Let

$$i_1 = \frac{1}{2}(\nabla^2 w)^2 - \frac{1}{2}(\nabla^2\psi)^2 - 4p\,H(\tau)\left(1 - \alpha\frac{x}{\lambda}\cos\theta\right) w - w''\left(\frac{1}{x}w' + \frac{1}{x^2}\ddot{w}\right)\psi$$

$$i_2 = \psi' w'$$

$$i_3 = \frac{1}{x^2}\dot{\psi}\dot{w}$$

$$i_4 = \psi\left[\left(\frac{1}{x}\dot{w}\right)'\right]^2$$

$$i_5 = -\frac{1}{2}\left[(1-\nu)(w')^2 - (1+\nu)(\psi')^2\right] \tag{19}$$

and assume that these integrands are constant over the elemental areas and length shown in Figure 2. Also, assume that $\overset{*}{w}$ is constant over the elemental area corresponding to i_1. Then summing up all the elemental areas we have approximately

$$T = \left\{\frac{N}{8}\overset{*}{w}_0^2 + \sum_{m=1}^{M} m\left[\frac{1}{2}\left(\overset{*}{w}_{m,0}^2 + \overset{*}{w}_{m,N}^2\right) + \sum_{n=1}^{N-1}\overset{*}{w}_{m,n}^2\right]\right\}\Delta x^2\Delta\theta \tag{20}$$

$$\begin{aligned} I = {} & \left\{\frac{N}{8}i_{1,0} + \sum_{m=1}^{M}\left[\frac{1}{2}\left(i_{1,m,0} + i_{1,m,N}\right) + \sum_{n=1}^{N-1} i_{1,m,n}\right]m\right\}\Delta x^2\Delta\theta \\ & + \sum_{m=0}^{M-1}\left[\frac{1}{2}\left(i_{2,m+1/2,0} + i_{2,m+1/2,N}\right) + \sum_{n=1}^{N-1} i_{2,m+1/2,n}\right]\left(m+\frac{1}{2}\right)\Delta x^2\Delta\theta \\ & + \frac{1}{2}\left[\frac{1}{2}\left(i_{2,M+1/2,0} + i_{2,M+1/2,N}\right) + \sum_{n=1}^{N-1} i_{2,M+1/2,n}\right]\left(M+\frac{1}{2}\right)\Delta x^2\Delta\theta \\ & + \sum_{m=1}^{M}\sum_{n=0}^{N-1}\frac{1}{m}\,i_{3,m,n+1/2}\,\Delta\theta \end{aligned}$$

$$+\sum_{m=0}^{M-1}\sum_{n=0}^{N-1} i_{4,m+1/2,n+1/2}\left(m+\frac{1}{2}\right)\Delta x^2\Delta\theta$$

$$+\left[\frac{1}{2}\left(i_{5,M+1/2,0}+i_{5,M+1/2,N}\right)+\sum_{n=1}^{N-1} i_{5,M+1/2,n}\right]\Delta\theta\ . \qquad (21)$$

Letting Z stand for either w or ψ we can express the derivatives in (21) in terms of the displacements and stress functions at the nodes of the finite difference net as follows

$$Z'_{m+1/2,n} = \frac{1}{\Delta x}\left(Z_{m+1,n}-Z_{m,n}\right)$$

$$\dot{Z}_{m,n+1/2} = \frac{1}{\Delta\theta}\left(Z_{m,n+1}-Z_{m,n}\right) \qquad (22)$$

$$(\nabla^2 Z)_{m,n} = \frac{1}{\Delta x^2}\left(Z_{m+1,n}-2Z_{m,n}+Z_{m-1,n}\right)$$

$$+\frac{1}{2x_m\Delta x}\left(Z_{m+1,n}-Z_{m-1,n}\right)$$

$$+\frac{1}{x_m^2\,\Delta\theta^2}\left(Z_{m,n+1}-2Z_{m,n}+Z_{m,n-1}\right)$$

$$\left(\frac{1}{x}\dot{Z}\right)'_{1/2,n+1/2} = \frac{1}{2\Delta x^2\Delta\theta}\left(w_{1,n+1}-w_{1,n}+w_{1,N-1-n}-w_{1,N-n}\right)$$

$$\left(\frac{1}{x}\dot{Z}\right)'_{m+1/2,n+1/2} = \frac{1}{\Delta x\Delta\theta}\left[\frac{1}{x_{m+1}}\left(Z_{m+1,n+1}-Z_{m+1,n}\right)-\frac{1}{x_m}\left(Z_{m,n+1}-Z_{m,n}\right)\right] \quad m\geq 1$$

$$Z_{1/2,n+1/2} = \frac{1}{4}\left(2Z_0+Z_{1,n}+Z_{1,n+1}\right)$$

$$Z_{m+1/2,n+1/2} = \frac{1}{4}\left(Z_{m,n}+Z_{m+1,n}+Z_{m,n+1}+Z_{m+1,n+1}\right) \quad m\geq 1.$$

At the pole

$$(\nabla^2 Z)_0 = Z_0'' = \text{constant and}$$

$$(\nabla^2 Z)_0 = -\frac{1}{\Delta x^2}\left[2Z_0 - \frac{1}{N}\left(Z_{1,0} + Z_{1,N} + 2\sum_{n=1}^{N-1} Z_{1,n}\right)\right] . \tag{23}$$

At the edge of the shell

$$Z_{M+1/2,n} = \frac{1}{2}(Z_{M,n} + Z_{M+1,n}) = 0 \tag{24}$$

and on the diameter of symmetry (n = 0, N)

$$Z_{m,n} = \frac{1}{2\Delta\theta}(Z_{m,n+1} - Z_{m,n-1}) = 0 . \tag{25}$$

Substitution of (22) - (25) into (21) yields an expression consisting of a linear part I_F, quadratic part I_L, and cubic part I_{NL}, in w and ψ at node points inside the boundary. Thus

$$I = I_F + I_L + I_{NL} . \tag{26}$$

Next we approximate the acceleration term in (18) by Houbolt's four point unconditionally stable backwards difference formula [8], [9]

$$\overset{**}{w}_{m,n,k} = \frac{1}{\Delta\tau^2}(2w_{m,n,k} - 5w_{m,n,k-1} + 4w_{m,n,k-2} - w_{m,n,k-3}) \quad k \geq 3 \tag{27}$$

$$\overset{**}{w}_{m,n,2} = \frac{2}{\Delta\tau^2}(w_{m,n,2} - 2w_{m,n,1}) - 4p\left(1 - \alpha\frac{x_m}{\lambda}\cos\theta_n\right)$$

$$\overset{**}{w}_{m,n,1} = \frac{6}{\Delta\tau^2} w_{m,n,1} - 8p\left(1 - \alpha\frac{x_m}{\lambda}\cos\theta_n\right)$$

where the time τ is represented at discrete points by

$$\tau_k = k\Delta\tau . \tag{28}$$

Substitution of (20), (26) and (27) into (17) results in a set of nonlinear algebraic equations for $Z_{m,n,k}$. To solve these equations by successive linearizations using Newton's procedure [4], expand (17) in Taylor series about the r^{th} iterate and keep only the first two terms

$$\frac{d}{d\tau}\left(\frac{\partial T}{\partial \overset{*r}{Z}_i} + \frac{\partial^2 T}{\partial \overset{*r}{Z}_i \partial \overset{*r}{Z}_j}\ \delta \overset{*r}{Z}_j\right) + \frac{\partial I}{\partial Z_i^r} + \frac{\partial^2 I}{\partial Z_i^r \partial Z_j^r}\ \delta Z_j^r = 0 \tag{29}$$

where

$$\delta Z_j^r = Z_j^{r+1} - Z_j^r \tag{30}$$

and Z_i includes all mesh variables. Then with

$$\begin{aligned}
\frac{\partial I_F}{\partial Z_i^r} &= -F_L \\
\frac{\partial I_L}{\partial Z_i^r} &= A_L Z^r \\
\frac{\partial I_{NL}}{\partial Z_i^r} &= F_{NL} \\
\frac{\partial^2 I_F}{\partial Z_i^r \partial Z_j^r} &= 0 \qquad (31) \\
\frac{\partial^2 I_L}{\partial Z_i^r \partial Z_j^r} &= A_L \\
\frac{\partial^2 I_{NL}}{\partial Z_i^r \partial Z_j^r} &= A_{NL} \\
\frac{d}{d\tau}\left(\frac{\partial T}{\partial \overset{*r}{Z}_i}\right) &= \overset{**r}{w}_{m,n,k} \\
\frac{d}{d\tau}\left(\frac{\partial^2 T}{\partial \overset{*r}{Z}_i \partial \overset{*r}{Z}_j}\ \delta \overset{*r}{Z}_j\right) &= \delta \overset{**r}{w}_{m,n,k}
\end{aligned}$$

and the proper grouping into A_D and F_D of terms resulting from Houbolt's formula, (29) gives the basic iteration formula at the k^{th} time station as

$$\begin{aligned}
[A_L + A_{NL} + A_D]\,\delta Z_k^r &= F_L - F_{NL} - F_{D;k} - [A_L + A_D]\,Z_k^r \qquad k \geq 3 \\
[A_L + A_{NL} + A_D]\,\delta Z_2^r &= 2F_L - F_{NL} - F_{D,2} - [A_L + A_D]\,Z_2^r \qquad k = 2 \\
[A_L + A_{NL} + 3A_D]\,\delta Z_1^r &= 3F_L - F_{NL} - [A_L + A_D]\,Z_1^r \qquad k = 1 .
\end{aligned} \tag{32}$$

Each of equations (32) may be written as

$$A\,\delta Z = F \tag{33}$$

where δZ and Z are ordered identically as follows:

$$Z = \begin{Bmatrix} Z_0 \\ Z_1 \\ \vdots \\ \vdots \\ Z_m \\ \vdots \\ \vdots \\ Z_M \end{Bmatrix} \qquad Z_0 = \begin{Bmatrix} w_0 \\ \psi_0 \end{Bmatrix} \qquad Z_m = \begin{Bmatrix} w_{m,0} \\ \psi_{m,0} \\ \vdots \\ \vdots \\ w_{m,n} \\ \psi_{m,n} \\ \vdots \\ \vdots \\ w_{m,N} \\ \psi_{m,N} \end{Bmatrix} \tag{34}$$

The equations are ordered in the same way as the unknowns with w and ψ corresponding to the equilibrium equation (1) and the compatibility equation (2), respectively.

The system (33) is banded. It may be partitioned and written in the block "five-diagonal" form:

$$C_0\delta Z_0 + D_0\delta Z_1 + E_0\delta Z_2 = F_0$$

$$D_0^T\,\delta Z_0 + C_1\delta Z_1 + D_1\delta Z_2 + E_1\delta Z_3 = F_1$$

$$E_0^T\delta Z_0 + D_1^T\delta Z_1 + C_2\delta Z_2 + D_2\delta Z_3 + E_2\delta Z_4 = F_2$$

$$E_{m-2}\delta Z_{m-2} + D_{m-1}^T\delta Z_{m-1} + C_m\delta Z_m + D_m\delta Z_{m+1} + E_m\delta Z_{m+2} = F_m$$

$$m = 3, 4, \ldots M-2$$

$$E_{M-3}\delta Z_{M-3} + D_{M-2}^T\delta Z_{M-2} + C_{M-1}\delta Z_{M-1} + D_{M-1}\delta Z_M = F_{M-1}$$

$$E_{M-2}\delta Z_{M-2} + D_{M-1}^T\delta Z_{M-1} + C_M\delta Z_M = F_M. \qquad (35)$$

where

$$C_m = C_{L,m} + C_{NL,m} + C_{D,m}$$

$$D_m = D_{L,m} + D_{NL,m}$$

$$E_m = E_{L,m}$$

$$F_m = F_{L,m} - F_{NL,m} - F_{D,m} - [E_{L,m-2}Z_{m-2} + D_{L,m-1}^T Z_{m-1} + (C_{L,m} + C_{D,m})Z_m + D_{L,m}Z_{m+1} + E_{L,m}Z_{m+2}]. \qquad (36)$$

The elements of $C_{L,m}, D_{L,m}, E_{L,m}, F_{L,m}, C_{NL,m}, D_{NL,m}, F_{NL,m}, C_{D,m}, F_{D,m}$ matrices are given in the Appendix.

The system of linear equations (35) is solved recursively using an extension of Potter's method [10].

$$\delta Z_m = -X_m\delta Z_{m+1} - Y_m\delta Z_{m+2} + Q_m. \qquad (37)$$

Expressions for the matrices X_m, Y_m, and Q_m may be obtained by substituting into (35). They are:

$$X_0 = C_0^{-1} D_0$$

$$Y_0 = C_0^{-1} E_0$$

$$Q_0 = C_0^{-1} F_0$$

$$X_1 = S_1 [D_1 - D_0^T Y_0]$$

$$Y_1 = S_1 E_1$$

$$Q_1 = S_1 [F_1 - D_0^T Q_0]$$

$$X_2 = S_2 [D_2 - (D_1 - E_0^T X_0) Y_1]$$

$$Y_2 = S_2 E_2$$

$$Q_2 = S_2 [F_2 - (D_1 - E_0^T X_0) Q_1 - E_0^T Q_0]$$

$$X_m = S_m [D_m - (D_{m-1} - E_{m-2} X_{m-2}) Y_{m-1}]$$

$$Y_m = S_m E_m$$

$$Q_m = S_m [F_m - (D_{m-1} - E_{m-2} X_{m-2}) Q_{m-1} - E_{m-2} Q_{m-2}]$$

$$m = 3, 4, \ldots M-1$$

except $Y_{M-1} = 0$

$$Z_M = S_M [F_M - (D_{M-1} - E_{M-2} X_{M-2}) Q_{M-1} - E_{M-2} Q_{M-2}]$$

where

$$S_1 = [C_1 - D_1^T X_0]^{-1}$$

$$S_2 = [C_2 - (D_1 - E_0^T X_0) Y_1 - E_0^T Y_0]^{-1} \qquad (38)$$

$$S_m = [C_m - (D_{m-1} - E_{m-2} X_{m-2}) Y_{m-1} - E_{m-2} Y_{m-2}]^{-1}$$

$$m = 2, 3, \ldots M .$$

COMPUTATION PROCEDURE

The characteristic deflection of the shell $\overline{V}$, referred to as volume of deformation is related to the deflection as follows

$$\overline{V} = \frac{\int_0^{2\pi}\int_0^{\lambda} W\, r\, dr\, d\theta}{\int_0^{2\pi}\int_0^{\lambda} \zeta r\, dr\, d\theta}$$

$$= \frac{8}{N\left(M+\frac{1}{2}\right)^2\lambda^2}\left\{\frac{N}{8}w_0 + \sum_{m=1}^{M} m\left[\frac{1}{2}w_{m,0} + \frac{1}{2}w_{m,n} + \sum_{n=1}^{N-1} w_{m,n}\right]\right\}. \tag{39}$$

The asymmetry of the deflection is measured by the difference in volume of deformation corresponding to the highly loaded region $0 \le r \le a$, $\pi/2 \le \theta \le \pi$, and lightly loaded region $0 \le r \le a$, $0 \le \theta \le \pi/2$

$$\overline{V}_D = \frac{8}{N\left(M+\frac{1}{2}\right)^2\lambda^2}\sum_{m=1}^{M} m\left[\frac{1}{2}w_{m,N} - \frac{1}{2}w_{m,0} + \sum_{n=\frac{N}{2}+1}^{N-1} w_{m,n} - \sum_{n=1}^{N/2-1} w_{m,n}\right]. \tag{40}$$

The computation procedure is summarized below.

1. Set up the linear coefficient matrix A_L, the dynamic matrix A_D, and the load matrix F_L.

2. Set all mesh variables Z to zero.

3. Compute the nonlinear coefficient matrix A_{NL}, the pseudo load matrices F_{NL} and F_D.

4. Solve the first of equations (32).

5. Add the increment δZ to the solution Z.

6. Repeat Steps 3 - 5 until solution has converged. The criterion for convergence is

$$\frac{\|\delta Z\|}{\|Z\|} \leq \epsilon \tag{41}$$

where $\|Z\| = \sqrt{\sum_{m,n} Z^2_{m,n}}$ and ϵ is a specified constant. This yields the solution at the first time station.

7. Extrapolate a starting solution for the next time station by applying

$$Z_k = 3Z_{k-1} - 3Z_{k-2} + Z_{k-3} \quad (k \geq 2,\ Z_0 = Z_{-1} = 0) \tag{42}$$

at every spatial finite difference mesh point.

8. Repeat Steps 3 - 6, except at Step 4 solve the second of equations (32). This yields the solution at the second time station.

9. To obtain the solution at the k^{th} ($k \geq 3$) time station, repeat Steps 7, and 3 - 6, except in Step 4 solve the third of equations (32).

10. Terminate the computation when solution is carried out to a specified time.

If at any time station the solution has not converged in a specified number of iterations, the iteration is stopped. The solution at the previous time station is taken for a starting iterate and Steps 3 - 6 are repeated. If convergence is achieved, Step 9 is repeated. If convergence is not achieved the computation is terminated.

The computation of the static load deflection curve and the determination of the static buckling load is a variant of the above computation procedure. Here we increment the load instead of the time. The applicable equations can be obtained from (32) by deleting the dynamic terms. The result is

$$[A_L + A_{NL}]\,\delta Z^r = F_L - F_{NL} - A_L Z^r \,. \tag{43}$$

A typical static load deflection curve is shown in Figure 3. The volume of deformation $\overline{V}$ increases with p. When p_{cr} is reached, the shell buckles and

$\overline{V}$ jumps from A to C. The AB branch of the load-deflection curve is unstable because the deformation increases with decreasing pressure.

The computation of the static load deflection curve is summarized below.

1. Set up the linear coefficient matrix A_L.
2. Set the load and all mesh variables Z to zero.
3. Increase the load by Δp and compute the load matrix.
4. Compute the nonlinear coefficient matrix A_{NL}.
5. Solve equation (43) and add the increment δZ to the solution Z.
6. Repeat Steps 4 and 5 until the solution converges according to (41).
7. Repeat Steps 3 - 6 until at some load level the solution fails to converge in a specified number of iterations.
8. Reduce the load by Δp and the load increment to $\eta \Delta p$, where $\eta < 1$.
9. Repeat Steps 3 - 7 with Δp replaced by $\eta \Delta p$.
10. Reduce the load by $\eta \Delta p$ and the initial load increment to $\eta^2 \Delta p$.
11. Repeat Steps 3 - 7 with Δp replaced by $\eta^2 \Delta p$.
12. When the solution fails to converge, it is assumed that the load level is near the relative maximum of the load-deflection curve. An attempt is then made to compute two points on the unstable branch of the load-deflection curve. The load is reduced by $2\eta^2 \Delta p$ and the starting iterate is taken to be

$$Z^{0}_{\ell-1} = Z_{\ell-1} + 5(Z_{\ell} - Z_{\ell-1}) \tag{44}$$

where Z_{ℓ} is the last converged solution. If the solution converges, the load is incremented by $\eta^2 \Delta p$. If the solution fails to converge, the computation is stopped.

The asymmetric linear static deformation is governed by

$$A_L Z = F_L . \tag{45}$$

It can be computed by that section of the dynamic computer program which solves linear simultaneous equations.

VALIDATION OF NUMERICAL METHOD

The validity of the numerical method is partly demonstrated by the results of the following special cases of the deformation of a simply supported shallow spherical shell:

1. Asymmetric linear static deformation, which provides a check on the two dimensional finite difference equations and the method of solving them;

2. Symmetric nonlinear static deformation and buckling, checking the application of Newton's method; and

3. Symmetric nonlinear dynamic deformation and buckling, checking Houbolt's method.

4. Asymmetric nonlinear static deformation and buckling.

The results of these computations are compared with results that are published or obtained with other computer programs.

Asymmetric Linear Static Deformation

The asymmetric linear static deformation of a shell with $\lambda = 8$, $p = 0.5$, $\nu = 0.3$ and $\alpha = 1.0$ was computed. A finite difference net with $M = 25$ and $N = 4$ was used. The deflections are compared in Figure 4 with those obtained with 100 finite difference stations from a published program [11]. The program [11] is based on the analysis of Reference 12. The example solution was computed with a Fortran program on the IBM 360/75 in approximately seven seconds. Thus the present analysis leads to an accurate and efficient solution of the asymmetric linear static problem.

Axisymmetric Nonlinear Static Deformation and Buckling

The axisymmetric buckling load for shells with $\lambda = 4$ and 8 subjected to uniform pressure ($\alpha = 0$) was computed. In both cases $\nu = 0.3$, initial $\Delta p = 0.05$,

M = 15, N = 4, and 7 iterations were permitted to achieve a converged solution at a given load level. For $\lambda = 4$ case, $\epsilon = 0.001$ and $\eta = 0.1$; for $\lambda = 8$ case, $\epsilon = 0.01$, $\eta = 0.2$. The critical pressures obtained in the present analysis are compared to those obtained by Weinitschke [13] and Schaeffer [7] below.

λ	4	8
p_{cr} present analysis	0.6615	0.796
p_{cr} Weinitschke [13]	0.660	0.791
p_{cr} Schaeffer [7]	0.646	0.857

The present buckling pressures are in very good agreement with those obtained by Weinitschke [13] and in reasonably good agreement with those obtained by Schaeffer [7]. The load deflection curves and the deformed shapes near the buckling pressures are shown in Figures 5 and 6.

These calculations do not consider possible bifurcation from the symmetric state of deformation. Weinitschke [14] has shown that bifurcation occurs for $\lambda > 4$.

Each load-deflection curve in Figure 5 was computed with a Fortran program on the CDC 6600 in approximately 2.5 minutes.

Axisymmetric Nonlinear Dynamic Response and Buckling

The dynamic buckling load for shells with $\lambda = 5$ subjected to uniform pressure of infinite duration was computed. Poisson's ratio $\nu = 0.3$, $\epsilon = 0.01$ and the finite difference net was such that M = 15, N = 4, and $\Delta\tau = 0.1$.

An ensemble of responses for various load amplitudes is shown in Figure 7. The maxima of these responses as a function of the load amplitude are presented in Figure 8. The load at which the response of the structure changes abruptly from "moderate to severe", from sub-critical to super-critical, is taken to be the dynamic buckling load [15]. Thus, for this case $p_{cr} = 0.57$ approximately. The deflected shapes at $\overline{V}_{max}$ for p = 0.55 and p = 0.6 are shown in Figure 9. Note that

at the super-critical load p = 0.60, the deflection at the pole is more than twice the initial rise H and the shell is in the "inverted" or inside-out position with all points on the shell below the base plane. At the sub-critical load p = 0.55 the shell has deformed only moderately.

The present results are in good agreement with those obtained from an analysis and program for the axisymmetric nonlinear dynamic response of shells of revolution developed at the NASA Langley Research Center and described in Reference 16. (See Figure 7.) The Langley results are for $\Delta\tau = 0.25$ and 25 finite difference stations along a meridian.

The present $p_{cr} = 0.57$ for a simply supported shell is higher than the $p_{cr} = 0.49$ computed by Huang [1] for a clamped shell. The ratio of dynamic to static buckling loads for shells with $\lambda = 5$ and clamped edge is 0.78 [1] [17]. For simply supported shells, the ratio is 0.76 based on symmetric static buckling and 0.91 based on the static load at bifurcation.

Asymmetric Nonlinear Static Deformation and Buckling

Static buckling loads for asymmetrically ($\alpha = 1$) loaded shells with $\lambda = 4$ and 8 were computed. For $\lambda = 4$, $\alpha = 1$, $\nu = 0.3$, $\Delta p = 0.05$, $\eta = 0.2$, $\epsilon = 0.01$, the finite difference nets used, the maximum number of iterations permitted at each load level, and the critical pressures are given below:

M	5	10	15	15
N	4	4	4	6
Iterations (maximum)	10	7	7	7
p_{cr}	0.316	0.328	0.332	0.328 .

The difference in the last three critical pressures is about 1%, indicating convergence of the finite difference net. The critical pressure is taken to be 0.328.

For $\lambda = 8$, $\alpha = 1$, $\nu = 0.3$, the parameters of the problem and the critical pressures are given below:

M	5	15	15	15
N	4	4	6	8
Iterations (maximum)	7	7	10	10
Δp	0.05	0.05	0.025	0.05
η	0.1	0.1	0.2	0.1
ϵ	0.001	0.01	0.001	0.0001
p_{cr}	0.3245	0.378	0.411*	0.425*.

In the computation of the critical pressures marked by an asterisk points on the unstable portion of the load deflection curve were not obtained. Since in these cases the failure of Newton's procedure to converge may be due to causes other than the non-existence of an adjacent equilibrium position on the stable branch of the load-deflection curve [18], these buckling pressures should be viewed with caution.

The load-deflection curves for $\lambda = 4$ and 8 and the deflections of these shells are shown in Figures 10-15. The slope of the $\lambda = 4$ load deflection curve decreases monotonically and the deflections at the buckling pressure of $p_{cr} = 0.328$ have essentially the same character as the load, that is, they contain mostly a uniform part and a $\cos\theta$ part. The slope of the $\lambda = 8$ load-deflection curve, however, decreases up to $p = 0.35$, increases slightly from 0.35 to 0.40 and then decreases again. The reversal of the change in slope is accompanied by drastic changes in the deflected shape of the shell as shown by Figures 12-15. At $p = 0.30$ the deflected shape contains mostly a uniform part and a $\cos\theta$ part. At $p = 0.35$ the deflected shape has a pronounced waviness in the θ direction near $\theta = \pi$ as shown in Figure 15. This is a plot of the deflections along the parallel $r/a = 0.71$ at which the deflection peaks in Figures 12-14 occur. At $p_{cr} = 0.425$ the shell has returned to a simpler shape than that at $p = 0.35$ but containing contributions from components higher than $\cos\theta$. The deflected shape at $p = 0.35$ appears to be associated with a local instability of the shell. It should be further investigated. Probably a finite difference net having $N > 8$ and smaller load increments should be used.

Asymmetric critical pressures for $\lambda = 4$ and 8, obtained with the program described in Reference 19 using 25 stations on the meridian and 8 terms in the Fourier expansion of the solution in the circumferential direction, are 0.336 and 0.304 respectively. Thus for $\lambda = 4$ the critical pressure for this analysis agrees very well with that obtained with the program of Reference 19. For $\lambda = 8$, the critical pressure obtained with the program of Reference 19, although much lower than that of the present analysis is close to the pressure associated with local instability.

The buckling pressures for asymmetrically loaded shells with $\lambda = 4$ and 8 are approximately 50% of those loaded axisymmetrically, although the total loads from the asymmetric and uniform loadings of equal intensity are the same. The membrane stresses at p_{cr} from the asymmetric load are also much lower than those from uniform pressure as shown in Figure 16. The stress resultants in Figure 16 are scaled with respect to the classical buckling stress:

$$\overline{N}_r = \frac{N_r}{\frac{1}{2} q_0 R}$$

$$\overline{N}_\theta = \frac{N_\theta}{\frac{1}{2} q_0 R} .$$

The ratio N_θ/N_r, however, is approximately the same for both uniformly and asymmetrically loaded shells.

ASYMMETRIC NONLINEAR DYNAMIC DEFORMATION AND BUCKLING

Asymmetric dynamic buckling loads for shells with $\lambda = 4, 6$, and 8 subjected to an asymmetric loading with $\alpha = 1$ were computed. The problem parameters are listed below:

λ	4	6	8
M	15	15	15
N	4	4	8
$\Delta\tau$	0.1	0.1	0.05
ϵ	0.01	0.01	0.01

The spatial finite difference nets for $\lambda = 4$ and 8 are those which gave accurate results in the calculation of asymmetric static buckling loads. The time increment was determined by trial and error. For $\lambda = 4$, $p = 0.4$ and $\tau^* = \infty$ responses were computed with $\Delta\tau = 0.1$ and 0.5. These differed by less than 10% and, therefore, $\Delta\tau = 0.1$ was used in all calculations with $\lambda = 4$ and 6. For $\lambda = 8$, $p = 0.2$, $\tau^* = \infty$ responses were computed with $\Delta\tau = 0.2$, 0.1, 0.05, and 0.025. The selected time increment $\Delta\tau = 0.05$ represents a compromise between accuracy and computing time.

Ensembles of response histories for $\lambda = 4$ and load durations of $\tau^* = 1, 5$ and ∞ are displayed in Figure 17. The dynamic load deflection curves for these cases are shown in Figure 18. For $\tau^* = 5$ and ∞ the transition from sub-critical to super-critical response occurs in a narrow load range and thus the dynamic buckling load is sharply defined. For $\tau^* = 1$, $\overline{V}_{max}$ increases gradually with the load intensity p. In this case p_{cr} is associated with the inflection point of the load deflection curve, as proposed in Reference 20. Note also that the time required to reach $\overline{V}_{max}$ increases as p approaches p_{cr} from below and then decreases as p increases above p_{cr}. For $\tau^* = 1$ the $p = 1.0$ response achieves its maximum later than all other presented. This places p_{cr} between 0.9 and 1.0 which is in agreement with the load at the inflection point of the load deflection curve. Thus the time to reach $\overline{V}_{max}$ can assist in the determination of p_{cr}.

The variation of p_{cr} and the critical impulse, $I_{cr} = p_{cr}\,\tau^*$, with τ^* and a comparison of static and dynamic buckling loads is shown in Figure 20. The lowest dynamic load, occurring when $\tau^* = \infty$, is 84% of the static p_{cr}.

Also presented in Figure 18 are $(\overline{V}_D)_{max}$ - p curves. $\overline{V}_D$ histories for $\tau^* = \infty$ are displayed in Figure 19. For this case, $(\overline{V}_D)_{max}$ increases sharply at the same load as $\overline{V}$, thus providing an alternate criterion for dynamic buckling. Based on $\overline{V}_D$ histories, the critical pressures for $\tau^* = 1$ and 5 are 0.65 and 0.30 respectively. Thus the $\overline{V}_D$ criterion leads to conservative buckling loads. For the present purpose, dynamic buckling loads are determined on the basis of $\overline{V}$.

The cross at the end of several response curves in Figure 17 indicates that Newton's procedure failed to converge at that point. Convergence failure is discussed at the end of this section.

Ensembles of response histories $\lambda = 6$, $\tau^* = 5$ and ∞ are displayed in Figure 21. The failure of Newton's procedure to converge does not allow the construction of the $\overline{V}_{max}$ - p curve for $\tau^* = \infty$. The dynamic buckling load in this case is determined from $\overline{V}_D$ histories shown in Figure 22. The dynamic load-deflection curves are shown in Figure 23.

As in the $\lambda = 4$, $\tau^* = \infty$ case, the transition from sub-critical to super-critical response for $\lambda = 6$, $\tau^* = \infty$ occurs in a narrow load range and the dynamic buckling load is well defined. In the $\tau^* = 5$ case the transition is more complex and the striking feature of the load-deflection curve is the presence of two inflection points. At the second inflection point, associated with p = 0.425, the shell has deformed to the inside out position. At the first inflection point, p = 0.395, severe deformation has occurred ($\overline{V} = 0.7$) and in addition V_D increases rapidly as shown in Figure 23. Thus the load, p = 0.395, associated with the first inflection point of the load-deflection curve is considered as the dynamic buckling load.

An ensemble of response histories for $\lambda = 8$, $\tau^* = 5$ is shown in Figure 24. The plot shows severe interference from convergence failures, but the dynamic buckling load can still be located near p = 0.39. The significant feature of the p = 0.39 curve is the slow development of the response which has not yet reached a maximum at $\tau = 30$.

A summary of buckling loads for simply supported shallow spherical shells is presented in Figure 25. The figure includes the static buckling loads due to uniform pressure obtained by Weinitschke [13][14] and Schaeffer [7] and the static and dynamic buckling loads due to uniform pressure and asymmetric loading obtained in the present investigation.

The asymmetric dynamic response described above was obtained with a Fortran program on the CDC 6600. In the $\lambda = 4$ and 6 cases one iteration required approximately 0.8 seconds of computer time, and in the $\lambda = 8$ case, 3.2 seconds. After the starting iterate at each time step was extrapolated using (42), only one iteration of Newton's procedure was generally required for a solution norm accurate to 1%. Thus, the remarkable feature of this computation procedure is its speed. Computer time required for large deflection, nonlinear response appears to be of the same order of magnitude as that needed for linear response.

In several instances Newton's procedure failed to converge (see curves marked by a cross in Figures 17, 21, and 24). This usually occurred abruptly without a gradual build-up of the number of iterations required for convergence. In all calculations five iterations were allowed to achieve a converged solution. The convergence failure of $\lambda = 4$, $p = 0.4$, $\tau^* = \infty$ (see Figure 17) was investigated in some detail. It was found that at the point of failure the corrections to the solution decreased in the first few iterations but then increased rapidly resulting in a diverging solution. Adding one fifth of the correction to the solution also resulted in convergence failure at the same point in time. Changing the time increment to 0.05, 0.2 and 0.5 and starting with the extrapolated iterate also resulted in convergence failure at the same time as shown in Figure 16. However using a time increment of $\Delta\tau = 0.5$, starting with the extrapolated iterate at all time steps and, after convergence failure, restarting with the solution at the last time step, a converged solution was obtained in this case. In this manner, the solution could be continued in several other cases but in many cases this approach also failed. Thus, it appears that in some instances the convergence of Newton's procedure is very sensitive to the starting iterate. The underlying causes of these convergence failures should be more thoroughly investigated so that a failure-free computation procedure can be designed.

CONCLUDING REMARKS

A numerical analysis and computer program are developed for the computation of the large deflection dynamic response of simply supported thin shallow spherical shells subjected to a class of spatially asymmetric and timewise step loadings. A variant of the program calculates large deflection static response and buckling loads. The numerical method employs timewise finite differences and two dimensional spatial finite differences. The latter are derived from the relative extremum of a definite integral. The solution is marched out in time by Houbolt's unconditionally stable backwards difference formula. At each time step the resulting nonlinear boundary value problem is solved by successive linearizations using Newton's procedure. The linear simultaneous equations of each linearization are solved recursively by an extension of Potters method. Computation times are considered reasonable for all cases computed.

For shells with $\lambda = 4$ and 8 the asymmetry of the loading reduces the static buckling loads to 50% and 53% of the corresponding symmetric buckling loads for uniform pressure. For $\lambda = 4$ the asymmetric dynamic buckling load of infinite duration is 84% of the corresponding static one. For load durations shorter than the period of oscillation of the shell ($\tau^* < 5$) the dynamic buckling loads are greater than the satic ones.

For $\lambda = 6$ and asymmetric loadings with durations of $\tau^* = 5$ and ∞, the dynamic buckling loads are 0.395 and 0.235 respectively. For $\lambda = 8$, $\tau^* = 5$, it is approximately 0.39.

ACKNOWLEDGMENT

The author thanks Drs. Robert E. Fulton and Wendell B. Stephens, NASA, Langley Research Center for computing comparison cases and acknowledges the helpful discussions with Professors John W. Hutchinson and D. G. M. Anderson, Harvard University.

Appendix

Sub-matrices of the Linear Coefficient Matrix A_L

$C_{L,0}(2 \times 2)$

$\frac{9N}{4}$	$\frac{1}{2}N\Delta x^2$
$\frac{1}{2}N\Delta x^2$	$-\frac{9N}{4}$

$D_{L,0}(2 \times \overline{N})$ $\quad (\overline{N} = 2N + 2)$

$-\frac{3}{2}$	$-\frac{1}{4}\Delta x^2$	←	←	-3	$-\frac{1}{2}\Delta x^2$	→	→	$-\frac{3}{2}$	$-\frac{1}{4}\Delta x^2$
$-\frac{1}{4}\Delta x^2$	$\frac{3}{2}$			$-\frac{1}{2}\Delta x^2$	3			$-\frac{1}{4}\Delta x^2$	$\frac{3}{2}$

$E_{L,0}(2 \times \overline{N})$

$\frac{3}{8}$	0	←	←	$\frac{3}{4}$	0	→	→	$\frac{3}{8}$	0
0	$-\frac{3}{8}$			0	$-\frac{3}{4}$			0	$-\frac{3}{8}$

$$C_{L,1} = C_{L,A} + C_{L,B}$$

$C_{L,A}(\overline{N} \times \overline{N})$

$$C_{L,A} = \frac{2}{N}$$

$\frac{1}{4}$	0			$\frac{1}{2}$	0			$\frac{1}{4}$	0
0	$-\frac{1}{4}$			0	$-\frac{1}{2}$			0	$-\frac{1}{4}$
				↑					
$\frac{1}{2}$	0	←		1	0	→		$\frac{1}{2}$	0
0	$-\frac{1}{2}$			0	-1			0	$-\frac{1}{2}$
				↓					
$\frac{1}{4}$	0			$\frac{1}{2}$	0			$\frac{1}{4}$	0
0	$-\frac{1}{4}$			0	$-\frac{1}{2}$			0	$-\frac{1}{4}$

$C_{L,B}(\overline{N} \times \overline{N})$

a	b	c	d	e									
b	-a	d	-c		-e								
c	d	g	h	c	d	e							
d	-c	h	-g	d	-c		-e						
		e		c	d	f	h	c	d	e			
			-e	d	-c	h	-f	d	-c		-e		
						e		c	d	g	h	c	d
							-e	d	-c	h	-g	d	-c
								e		c	d	a	b
									-e	d	-c	b	-a

$$a = \frac{9}{16} + \frac{1}{\Delta\theta^4} + 2\left(1 + \frac{1}{\Delta\theta^2}\right)^2$$

$$b = \Delta x^2 \left(1 + \frac{1}{\Delta\theta^2}\right)$$

$$c = -\frac{4}{\Delta\theta^2} \left(1 + \frac{1}{\Delta\theta^2}\right)$$

$$d = -\frac{\Delta x^2}{\Delta\theta^2}$$

$$e = \frac{1}{\Delta\theta^4}$$

$$f = 2a$$

$$g = f + e$$

$$h = 2b$$

The size and structure of the $C_{L,m}$ ($m = 2, 3, \ldots M$) matrices are the same as those of the $C_{L,B}$ matrix. The elements follow for $m = 2, 3 \ldots M-1$

$$a = 3m\left(1 + \frac{1}{m^4\Delta\theta^4}\right) + \frac{4}{m\Delta\theta^2} + \frac{m}{4(m^2-1)}$$

$$b = m\Delta x^2\left(1 + \frac{1}{m^2\Delta\theta^2}\right)$$

$$c = -\frac{4}{m\Delta\theta^2}\left(1 + \frac{1}{m^2\Delta\theta^2}\right)$$

$$d = -\frac{\Delta x^2}{m\Delta\theta^2}$$

$$e = \frac{1}{m^3\Delta\theta^4}$$

$$f = 2a$$

$$g = f + e$$

$$h = 2b$$

For $m = M$

$$a = \frac{1}{2}(M-1)\left[1 + \frac{1}{2(M-1)}\right]^2 + \frac{1}{2}M\left(3 + \frac{1}{2M} + \frac{2}{M^2\Delta\theta^2}\right) + \frac{1}{M^3\Delta\theta^4} - 2(1-\nu)$$

$$b = \frac{1}{2}M\Delta x^2\left(3 + \frac{1}{2M} + \frac{2}{M^2\Delta\theta^2}\right)$$

$$c = -\frac{2}{M\Delta\theta^2}\left(3 + \frac{1}{2M} + \frac{2}{M^2\Delta\theta^2}\right)$$

$$d = -\frac{\Delta x^2}{M\Delta\theta^2}$$

$$e = \frac{1}{M^3\Delta\theta^4}$$

$$f = 2a$$

$$g = f + e$$

$$h = 2b$$

$D_{L,m}(\overline{N} \times \overline{N})$ $\quad m = 1,2, \ldots\ldots M-1$

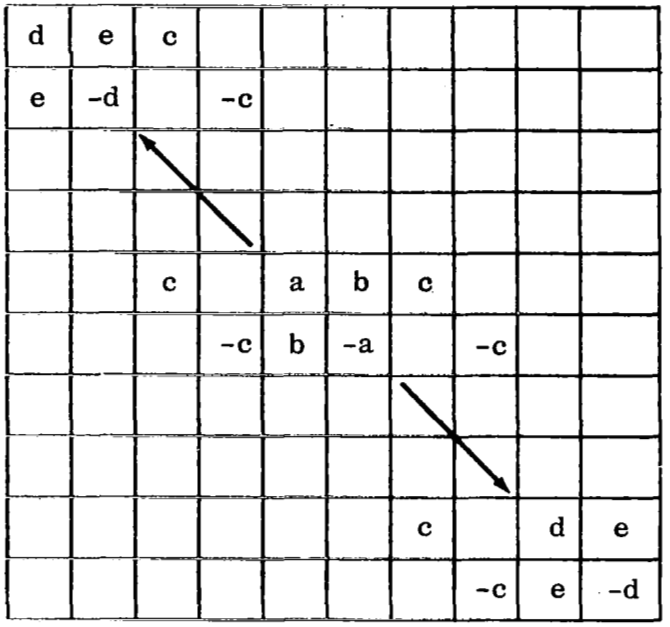

For $m = 1,2 \ldots . M-2$:

$$a = -\frac{2}{\Delta\theta^2}\left(m + \frac{1}{2}\right)\left[2\Delta\theta^2 + \frac{1}{m^2} + \frac{1}{(m+1)^2}\right]$$

$$b = -\Delta x^2\left(m + \frac{1}{2}\right)$$

$$c = \frac{1}{\Delta\theta^2}\left(m + \frac{1}{2}\right)\left[\frac{1}{m^2} + \frac{1}{(m+1)^2}\right]$$

$$d = \frac{1}{2}a$$

$$e = \frac{1}{2}b$$

$$D_{L,\,M-1} = \left[D_{L,m} - E_{L,m}\right]_{m = M-1}$$

$E_{L,m}(\overline{N} \times \overline{N})$ $\qquad\qquad$ $m = 1,2,\ldots.M-2$

$E_{L,m}$ is a diagonal matrix with the following elements:

$$E_{L,m,\,1,1} = \frac{1}{2}a$$

$$E_{L,m,\,2,2} = -\frac{1}{2}a$$

$$E_{L,m,2n+1,2n+1} = a$$

$$E_{L,m,2n+2,2n+2} = -a \qquad n = 1,2,\ldots.N-1$$

$$E_{L,m,2N+1,2N+1} = \frac{1}{2}a$$

$$E_{L,m,2N+2,2N+2} = -\frac{1}{2}a$$

$$a = m + 1 - \frac{1}{4(m+1)}$$

Sub-matrices of the Load Matrix F_L

$F_{L,0}(1 \times 2)$

f_1
0

$$f_1 = \frac{1}{2} Np\Delta x^4$$

$F_{L,m}(1 \times \overline{N})$ $\quad m = 1, 2, \ldots . M$

f_1
0
↑
f_n
0
↓
f_{N+1}
0

$$f_1 = 2p\Delta x^4 m \left(1 - \frac{m}{M + \frac{1}{2}}\right)$$

$$f_n = 4p\Delta x^4 m \left[1 - \frac{m}{M + \frac{1}{2}} \cos (n - 1)\,\Delta\theta\right] \quad n = 2,3,\ldots N$$

$$f_{N+1} = 2p\Delta x^4 m \left(1 + \frac{m}{M + \frac{1}{2}}\right)$$

Sub-matrices of the Nonlinear Coefficient Matrix A_{NL}

$C_{NL,0}(2 \times 2)$

a	b
b	0

$$a = -N\psi_0 + \frac{1}{2} S_1$$

$$b = -NS_2$$

$D_{NL,0}(2 \times \overline{N})$

$\frac{1}{2}a_0$	$\frac{1}{2}b_0$	←		a_n	b_n	→		$\frac{1}{2}a_N$	$\frac{1}{2}b_N$
$\frac{1}{2}c_0$	0			c_n	0			$\frac{1}{2}c_N$	0

$$a_n = \psi_0 - \psi_{1,n} - \frac{1}{\Delta\theta^2} \ddot{\psi}_{1,n}$$

$$b_n = W_0 - W_{1,n} - \frac{1}{\Delta\theta^2} \ddot{W}_{1,n}$$

$$c_n = S_2 - \frac{1}{4\Delta\theta^2} (\ddot{W}_{1,n} + \ddot{W}_{1,N-n})$$

$$C_{NL,1} = C_{NL,A} + C_{NL,B} + C_{NL,C}$$

$C_{NL,A}(\overline{N} \times \overline{N})$

$C_{NL,A} = -\frac{1}{N}\psi_0$

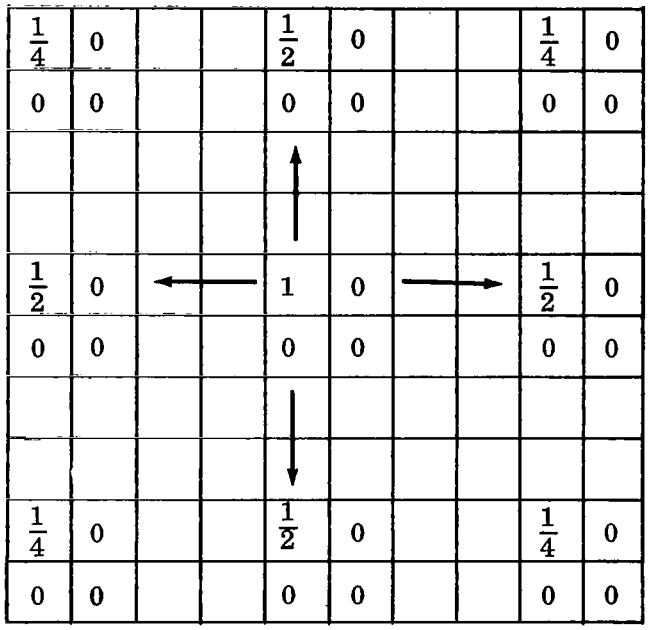

$C_{NL,B}(\overline{N} \times \overline{N})$

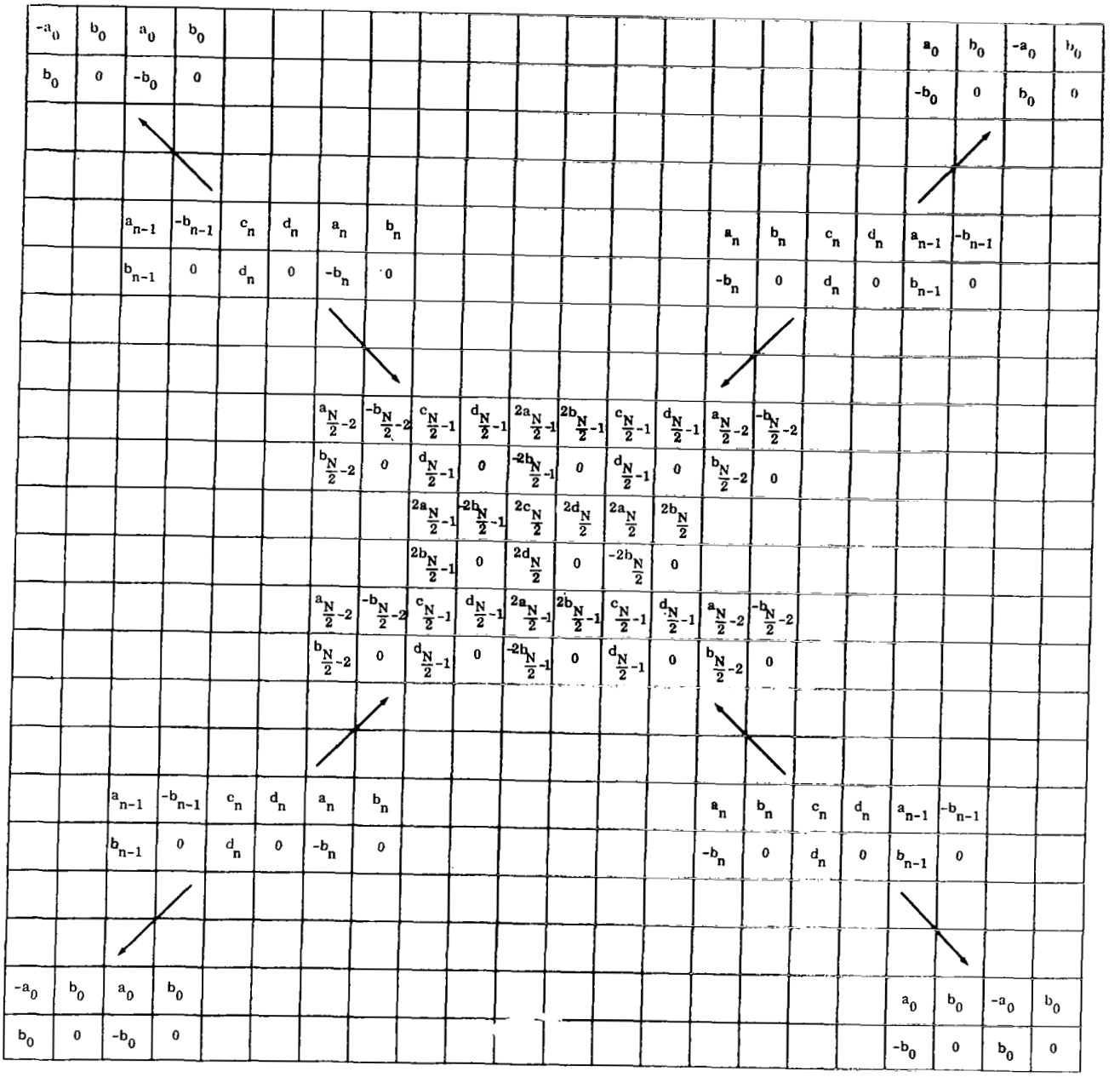

$$a_n = -\frac{1}{16\Delta\theta^2}\left(4\psi_0 + \psi_{1,n} + \psi_{1,n+1} + \psi_{1,N-1-n} + \psi_{1,N-n}\right)$$

$$b_n = -\frac{1}{16\Delta\theta^2}\left(W_{1,n+1} - W_{1,n} + W_{1,N-1-n} - W_{1,N-n}\right)$$

$$c_n = -\left(a_n + a_{n-1}\right)$$

$$d_n = b_n - b_{n-1}$$

$C_{NL,C}(\overline{N} \times \overline{N})$

a_0	b_0	c_1	d_1						
b	0	e_1	0						
		c_n	e_n	f_n	g_n	c_{n+1}	d_{n+1}		
		d_n	0	g_n	0	e_{n+1}	0		
						c_N	e_N	a_N	b_N
						d_N	0	b_N	0

$$a_{\substack{0\\N}} = \frac{1}{2}\psi_{2,\substack{0\\N}} + \frac{1}{\Delta\theta^2}\left(-4\psi_{1,\substack{0\\N}} + 3\psi_{3/2,\ 1/2\ \\ N-1/2}\right)$$

$$b_{\substack{0\\N}} = \frac{1}{2}\left(W_{2,\substack{0\\N}} - W_0\right) + \frac{1}{\Delta\theta^2}\left(\ddot{W}_{1,\substack{0\\N}} + W''_{1,\substack{0\\N}} \pm \frac{3}{4}\dot{W}'_{3/2,\ 1/2\ \\ N-1/2}\right)$$

$$\left.\begin{aligned} c_n &= \frac{2}{\Delta\theta^2}\left(\psi_{1,n-1} + \psi_{1,n} - \frac{3}{2}\psi_{3/2,n-1/2}\right) \\ d_n &= -\frac{1}{\Delta\theta^2}\left(W''_{1,n} - \frac{3}{4}\dot{W}'_{3/2,\ n-1/2}\right) \\ e_n &= -\frac{1}{\Delta\theta^2}\left(W''_{1,n-1} + \frac{3}{4}\dot{W}'_{3/2,n-1/2}\right) \end{aligned}\right\} n = 1, 2, \ldots . N$$

$$\left.\begin{aligned} f_n &= \psi_{2,n} + \frac{1}{\Delta\theta^2}\left[-8\psi_{1,n} + 3\left(\psi_{3/2,n-1/2} + \psi_{3/2,n+1/2}\right)\right] \\ g_n &= W_{2,n} - W_0 + \frac{1}{\Delta\theta^2}\left(2W''_{1,n} + 2\ddot{W}_{1,n} + \frac{3}{4}\dot{W}'_{3/2,n+1/2} - \frac{3}{4}\dot{W}'_{3/2,n-1/2}\right) \end{aligned}\right\} n=1, 2, \ldots N-1$$

In the expressions for $a_{\substack{0\\N}}$ and $b_{\substack{0\\N}}$ the two level subscript and sign should be interpreted as follows: to obtain the equation for a_0, drop the lower level sign and subscript on all symbols; for a_N replace the upper level subscript and sign by the lower level one.

The size and structure of the $C_{NL,\,m}$ ($m = 2, 3, \ldots M$) matrices are the same as those of the $C_{NL,\,C}$ matrix. The elements for $m = 2, 3, \ldots M-1$ follow.

$$a_{0_N} = \frac{1}{2}\left(\psi_{m+1,0_N} - \psi_{m-1,0_N}\right) + \frac{2}{m^2\Delta\theta^2}\left[-2m\,\psi_{m,0_N} + \left(m-\tfrac{1}{2}\right)\psi_{m-1/2,1/2_{N-1/2}} + \left(m+\tfrac{1}{2}\right)\psi_{m+1/2,1/2_{N-1/2}}\right]$$

$$b_{0_N} = \frac{1}{2}\left(W_{m+1,0_N} - W_{m-1,0_N}\right) + \frac{1}{m\Delta\theta^2}\left[\ddot{W}_{m,0_N} + W''_{m,0_N} \mp \tfrac{1}{2}\left(m-\tfrac{1}{2}\right)\dot{W}'_{m-1/2,1/2_{N-1/2}} \pm \tfrac{1}{2}\left(m+\tfrac{1}{2}\right)\dot{W}'_{m+1/2,1/2_{N-1/2}}\right]$$

$$\left.\begin{aligned} c_n &= \frac{2}{m^2\Delta\theta^2}\left[m\,\psi_{m,n-1} + m\psi_{m,n} - \left(m-\tfrac{1}{2}\right)\psi_{m-1/2,n-1/2} - \left(m+\tfrac{1}{2}\right)\psi_{m+1/2,n-1/2}\right] \\ d_n &= \frac{1}{m\Delta\theta^2}\left[-W''_{m,n} - \tfrac{1}{2}\left(m-\tfrac{1}{2}\right)\dot{W}'_{m-1/2,n-1/2} + \tfrac{1}{2}\left(m+\tfrac{1}{2}\right)\dot{W}'_{m+1/2,n-1/2}\right] \\ e_n &= \frac{1}{m\Delta\theta^2}\left[-W''_{m,n-1} + \tfrac{1}{2}\left(m-\tfrac{1}{2}\right)\dot{W}'_{m-1/2,n-1/2} - \tfrac{1}{2}\left(m+\tfrac{1}{2}\right)\dot{W}'_{m+1/2,n-1/2}\right] \end{aligned}\right\} n = 1, 2, \ldots N$$

$$\left.\begin{aligned} f_n &= \psi_{m+1,n} - \psi_{m-1,n} + \frac{2}{m^2\Delta\theta^2}\left[-4m\,\psi_{m,n} + \left(m-\tfrac{1}{2}\right)\left(\psi_{m-1/2,n-1/2} + \psi_{m-1/2,n+1/2}\right) + \left(m+\tfrac{1}{2}\right)\left(\psi_{m+1/2,n-1/2} + \psi_{m+1/2,n+1/2}\right)\right] \\ g_n &= W_{m+1,n} - W_{m-1,n} + \frac{1}{2m\Delta\theta^2}\left[4W''_{m,n} + 4\ddot{W}_{m,n} - \left(m-\tfrac{1}{2}\right)\left(\dot{W}'_{m-1/2,n+1/2} - \dot{W}'_{m-1/2,n-1/2}\right) + \left(m+\tfrac{1}{2}\right)\left(\dot{W}'_{m+1/2,n+1/2} - \dot{W}'_{m+1/2,n-1/2}\right)\right] \end{aligned}\right\} n = 1, 2, \ldots N-1$$

For m = M

$$a_{\substack{0\\N}} = -\frac{1}{2}\left(3\psi_{M,\substack{0\\N}} + \psi_{M-1,\substack{0\\N}}\right) + \frac{2}{M^2\Delta\theta^2}\left[-3M\psi_{M,\substack{0\\N}} + \left(M-\frac{1}{2}\right)\psi_{M-1/2,\substack{1/2\\N-1/2}}\right]$$

$$b_{\substack{0\\N}} = -\frac{1}{2}\left(3W_{M,0} + W_{M-1,0}\right) + \frac{1}{M\Delta\theta^2}\left[\frac{3}{2}\ddot{W}_{M,\substack{0\\N}} + W''_{M,\substack{0\\N}} + \frac{1}{2}\left(M-\frac{1}{2}\right)\dot{W}'_{M-1/2,\substack{1/2\\N-1/2}}\right]$$

$$\left.\begin{aligned} c_n &= \frac{2}{M^2\Delta\theta^2}\left[\frac{3}{2}M\left(\psi_{M,n-1} + \psi_{M,n}\right) - \left(M-\frac{1}{2}\right)\psi_{M-1/2,n-1/2}\right] \\ d_n &= \frac{1}{M\Delta\theta^2}\left[-W''_{M,n} - \frac{1}{2}\left(M-\frac{1}{2}\right)\dot{W}'_{M-1/2,n-1/2}\right] \\ e_n &= \frac{1}{M\Delta\theta^2}\left[-W''_{M,n-1} + \frac{1}{2}\left(M-\frac{1}{2}\right)\dot{W}'_{M-1/2,n-1/2}\right] \end{aligned}\right\} n=1,2,\ldots N$$

$$\left.\begin{aligned} f_n &= -3\psi_{M,n} - \psi_{M-1,n} + \frac{2}{M^2\Delta\theta^2}\left[-6M\psi_{M,n} + \left(M-\frac{1}{2}\right)\left(\psi_{M-1/2,n-1/2} + \psi_{M-1/2,n+1/2}\right)\right] \\ g_n &= -3W_{M,n} - W_{M-1,n} + \frac{1}{2M\Delta\theta^2}\left[4W''_{M,n} + 6\ddot{W}_{M,n} - \left(M-\frac{1}{2}\right)\left(\dot{W}'_{M-1/2,n+1/2} - \dot{W}'_{M-1/2,n-1/2}\right)\right] \end{aligned}\right\}$$

$n=1,2,\ldots N-1$

$D_{NL,m}(\bar{N} \times \bar{N})$ $\quad m = 1, 2, \ldots M-1$

a_0	b_0	c_0	d_1						
$\frac{1}{2}e_0$	0	f_1	0						
		↘							
			↘						
		g_n	$-d_n$	h_n	i_n	c_n	d_{n+1}		
		$-f_n$	0	e_n	0	f_{n+1}	0		
						↘			
							↘		
						g_N	$-d_N$	a_N	b_N
						$-f_N$	0	$\frac{1}{2}e_N$	0

$$a_0 = -\frac{1}{2}\left(\psi_{m+1,0} - \psi_{m,0}\right) + \frac{1}{m(m+1)\Delta\theta^2}\left[(m+1)\psi_{m,0} + m\psi_{m+1,0} - 2\left(m+\frac{1}{2}\right)\psi_{m+1/2,1/2}\right]$$
$N \qquad N \qquad N \qquad N \qquad N-1/2$

$$b_0 = -\frac{1}{2}\left(W_{m+1,0} - W_{m,0}\right) + \frac{1}{2m(m+1)\Delta\theta^2}\left[-m\ddot{W}_{m+1,0} \pm \left(m+\frac{1}{2}\right)(m+1)\,\dot{W}'_{m+1/2,1/2}\right]$$
$N \qquad N \qquad N \qquad N \qquad N-1/2$

$$c_n = -\frac{1}{m(m+1)\Delta\theta^2}\left[(m+1)\psi_{m,n+1} + m\psi_{m+1,n} - 2\left(m+\frac{1}{2}\right)\psi_{m+1/2,n+1/2}\right] \qquad n = 0, 1, 2, \ldots N-1$$

$$d_n = \frac{m+\frac{1}{2}}{2m\Delta\theta^2}\,\dot{W}'_{m+1/2,n-1/2} \qquad n = 1, 2, \ldots N$$

$$e_n = -\left(W_{m+1,n} - W_{m,n}\right) - \frac{1}{2m(m+1)^2\Delta\theta^2}\left[(m+1)\left(m+\frac{3}{2}\right)\ddot{W}_{m,n} + m\left(m+\frac{1}{2}\right)\ddot{W}_{m+1,n}\right] \qquad n = 0, 1, 2, \ldots N$$

$$f_n = \frac{m+\frac{1}{2}}{2(m+1)\Delta\theta^2}\,\dot{W}'_{m+1/2,n-1/2} \qquad n = 1, 2, \ldots N$$

$$g_n = -\frac{1}{m(m+1)\Delta\theta^2}\left[(m+1)\psi_{m,n-1} + m\psi_{m+1,n} - 2\left(m+\frac{1}{2}\right)\psi_{m+1/2,n-1/2}\right] \qquad n = 1, 2, \ldots N$$

$$\left.\begin{aligned} h_n &= -\left(\psi_{m+1,n} - \psi_{m,n}\right) + \frac{2}{m(m+1)\Delta\theta^2}\left[(m+1)\psi_{m,n} + m\psi_{m+1,n} - \left(m+\frac{1}{2}\right)\left(\psi_{m+1/2,n-1/2} + \psi_{m+1/2,n+1/2}\right)\right] \\ i_n &= -\left(W_{m+1,n} - W_{m,n}\right) - \frac{1}{(m+1)\Delta\theta^2}\left[\ddot{W}_{m+1,n} + \frac{1}{2m}\left(m+\frac{1}{2}\right)(m+1)\left(\dot{W}'_{m+1/2,n-1/2} - \dot{W}'_{m+1/2,n+1/2}\right)\right] \end{aligned}\right\} \qquad n = 1, 2, \ldots N-1$$

The expressions for W'', $\ddot{W}$, $\dot{W}'$, and $\ddot{\psi}$ in this appendix are different from those in the text. With Z representing ψ or W, they are:

$$\left.\begin{aligned} Z''_{m,n} &= Z_{m+1} - 2Z_{m,n} + Z_{m-1,n} \qquad m = 2,3,\ldots M-1 \\ Z''_{1,n} &= Z_{2,n} - 2Z_{1,n} + Z_0 \\ Z''_{M,n} &= -3Z_{M,n} + Z_{M-1,n} \end{aligned}\right\} n=0,1,2,\ldots N$$

$$\left.\begin{aligned} \ddot{Z}_{m,n} &= Z_{m,n+1} - 2Z_{m,n} + Z_{m,n-1} \qquad n = 1,2,\ldots N-1 \\ \ddot{Z}_{m,0} &= 2(Z_{m,1} - Z_{m,0}) \\ \ddot{Z}_{m,N} &= 2(Z_{m,N-1} - Z_{m,N}) \end{aligned}\right\} m=1,2,\ldots M$$

$$\dot{W}'_{m+1/2,n+1/2} = \frac{1}{m+1}\left(W_{m+1,n+1} - W_{m+1,n}\right) - \frac{1}{m}\left(W_{m,n+1} - W_{m,n}\right) \quad \begin{matrix} m=1,2,\ldots M-1 \\ n=0,1,2,\ldots N-1 \end{matrix}$$

$$\psi_{m+1/2,n+1/2} = \frac{1}{4}\left(\psi_{m,n} + \psi_{m,n+1} + \psi_{m+1,n+1} + \psi_{m+1,n}\right)$$

The following quantities also appear in expressions for matrix elements:

$$S_1 = \psi_{1,0} + \psi_{1,N} + 2\sum_{n=1}^{N-1} \psi_{1,n}$$

$$S_2 = W_0 - \frac{1}{2N}\left(W_{1,0} + W_{1,N} + 2\sum_{n=1}^{N-1} W_{1,n}\right)$$

$$S_4 = \psi_{1,0}W_{1,0} + \psi_{1,N}W_{1,N} + 2\sum_{n=1}^{N-1} \psi_{1,n}W_{1,n}$$

$$S_5 = \psi_{1,0}W_{1,1} + \psi_{1,N}W_{1,N-1} + \sum_{n=1}^{N-1} \psi_{1,n}\left(W_{1,n+1} + W_{1,n-1}\right)$$

Sub-matrices of the Pseudo Load Matrix F_{NL}

$F_{NL,0}(1 \times 2)$

$$f_1 = \frac{1}{2} W_0 S_1 - N\psi_0 S_2 + \left(\frac{1}{\Delta\theta^2} - \frac{1}{2}\right) S_4 - \frac{1}{\Delta\theta^2} S_5$$

$$f_2 = -\frac{1}{2} N S_2^2$$

$F_{NL,1}(1 \times \overline{N})$

$$f_{1,0}^{N} = \frac{1}{2}\psi_0 S_2 + \frac{1}{2}\psi_{1,0}^{N}\left(W_{2,0}^{N} - W_0\right) + \frac{1}{2}\psi_{2,0}^{N}\left(W_{1,0}^{N} - W_{2,0}^{N}\right)$$

$$- \frac{1}{\Delta\theta^2}\left[-\psi_{1,0}^{N}\left(W''^{N}_{1,0} + \ddot{W}^{N}_{1,0}\right) + \psi_{1,1}^{N-1} W''^{N-1}_{1,1} + \frac{1}{4}\psi_{2,0}^{N}\ddot{W}^{N}_{2,0} \mp 3\psi_{3/2,1/2}^{N-1/2}\dot{W}'^{N-1/2}_{3/2,1/2}\right]$$

$$f_{2,0}^{N} = -\frac{1}{4} W_{1,0}^{N}\left(W_{2,0}^{N} - W_0\right) + \frac{1}{4\Delta\theta^2}\left[-2W''^{N}_{1,0}\ddot{W}^{N}_{1,0} + \frac{3}{2}\left(\dot{W}'\right)^2_{3/2,1/2}\right]^{N-1/2}$$

$$f_{1,n} = \psi_0 S_2 + \psi_{1,n}\left(W_{2,n} - W_0\right) + \psi_{2,n}\left(W_{1,n} - W_{2,n}\right)$$

$$- \frac{1}{\Delta\theta^2}\left[\psi_{1,n-1} W''_{1,n-1} - 2\psi_{1,n}\left(W''_{1,n} + \ddot{W}_{1,n}\right) + \psi_{1,n+1} W''_{1,n+1} + \frac{1}{2}\psi_{2,n}\ddot{W}_{2,n}\right.$$

$$\left. + 3\left(\psi\dot{W}'\right)_{3/2,n-1/2} - 3\left(\psi\dot{W}'\right)_{3/2,n+1/2}\right]$$

$$f_{2,n} = -\frac{1}{2} W''_{1,n}\left(W_{2,n} - W_0\right) + \frac{1}{2\Delta\theta^2}\left[-2W''_{1,n}\ddot{W}_{1,n} + \frac{3}{4}\left(\dot{W}'\right)^2_{3/2,n-1/2} + \frac{3}{4}\left(\dot{W}'\right)^2_{3/2,n+1/2}\right]$$

$$n = 1, 2, \ldots N-1$$

The size and structure of the $F_{NL,m}$ ($m = 2,3,\ldots M$) matrices are the same as those of the $F_{NL,1}$ matrix. The elements for $m = 2,3,\ldots M-1$ follow.

$$f_{1,0}_{N} = -\frac{1}{2}\psi_{m-1,0}\,(W_{m,0} - W_{m-1,0})_{N} + \frac{1}{2}\psi_{m,0}\,(W_{m+1,0} - W_{m-1,0})_{N} + \frac{1}{2}\psi_{m+1,0}\,(W_{m,0} - W_{m+1,0})_{N}$$

$$- \frac{1}{m\Delta\theta^2}\left[\frac{m}{2(m-1)}\,\psi_{m-1,0}\,\ddot{W}_{m-1,0} - \psi_{m,0}\,(\ddot{W}_{m,0} + W''_{m,0})_{N} + \psi_{m,1}\,W''_{m,1}{}_{N-1}\right.$$

$$+ \frac{m}{2(m+1)}\,\psi_{m+1,0}\,\ddot{W}_{m+1,0} \pm 2\left(m-\tfrac{1}{2}\right)\psi_{m-1/2,1/2}\,\dot{W}'_{m-1/2,1/2}{}_{N-1/2}$$

$$\left. \mp 2\left(m+\tfrac{1}{2}\right)\psi_{m+1/2,1/2}\,\dot{W}'_{m+1/2,1/2}{}_{N-1/2}\right]$$

$$f_{2,0} = -\tfrac{1}{4}W''_{m,0}\,(W_{m+1,0} - W_{m-1,0})_{N} + \frac{1}{4\Delta\theta^2}\left[-\frac{2}{m}\,W''_{m,0}\,\ddot{W}_{m,0} + \left(m-\tfrac{1}{2}\right)(\dot{W}')^2_{m-1/2,1/2} + \left(m+\tfrac{1}{2}\right)(\dot{W}')^2_{m+1/2,1/2}{}_{N-1/2}\right]$$

$$f_{1,n} = -\psi_{m-1,n}\,(W_{m,n} - W_{m-1,n}) + \psi_{m,n}\,(W_{m+1,n} - W_{m-1,n}) + \psi_{m+1,n}\,(W_{m,n} - W_{m+1,n})$$

$$- \frac{1}{m\Delta\theta^2}\left\{\frac{m}{m-1}\,\psi_{m-1,n}\ddot{W}_{m-1,n} + \psi_{m,n-1}W''_{m,n-1} - 2\psi_{m,n}\,(W''_{m,n} + \ddot{W}_{m,n}) + \psi_{m,n+1}W''_{m,n+1}\right.$$

$$+ \frac{m}{m+1}\,\psi_{m+1,n}\ddot{W}_{m+1,n} - 2\left(m-\tfrac{1}{2}\right)\left[(\psi\dot{W}')_{m-1/2,n-1/2} - (\psi\dot{W}')_{m-1/2,n+1/2}\right]$$

$$\left. + 2\left(m+\tfrac{1}{2}\right)\left[(\psi\dot{W}')_{m+1/2,n-1/2} - (\psi\dot{W}')_{m+1/2,n+1/2}\right]\right\}$$

$$f_{2,n} = -\tfrac{1}{2}W''_{m,n}\,(W_{m+1,n} - W_{m-1,n}) + \frac{1}{4\Delta\theta^2}\left\{-\frac{4}{m}\,W''_{m,n}\ddot{W}_{m,n} + \left(m-\tfrac{1}{2}\right)\left[(\dot{W}')^2_{m-1/2,n-1/2} + (\dot{W}')^2_{m-1/2,n+1/2}\right]\right.$$

$$\left. + \left(m+\tfrac{1}{2}\right)\left[(\dot{W}')^2_{m+1/2,n-1/2} + (\dot{W}')^2_{m+1/2,n+1/2}\right]\right\}$$

$$n = 1,2,\ldots N-1$$

For m = M

$$f_{1,0}^{N} = -\frac{1}{2}\psi_{M-1,0}^{N}\left(W_{M,0}^{N} - W_{M-1,0}^{N}\right) - \frac{1}{2}\psi_{M,0}^{N}\left(3W_{M,0}^{N} + W_{M-1,0}^{N}\right)$$

$$- \frac{1}{M\Delta\theta^2}\left[\frac{M}{M-1}\psi_{M-1,0}^{N}\left(W_{M-1,1}^{N-1} - W_{M-1,0}^{N}\right) - 3\psi_{M,0}^{N}\left(W_{M,1}^{N-1} - W_{M,0}^{N}\right) - \psi_{M,0}^{N} W''^{N}_{M,0}\right.$$

$$\left. + \psi_{M,1}^{N-1} W''^{N-1}_{M,1} \pm 2\left(M - \frac{1}{2}\right)\left(\psi\dot{W}'\right)_{M-1/2,\,1/2}^{N-1/2}\right]$$

$$f_{2,0}^{N} = \frac{1}{4} W''^{N}_{M,0}\left(W_{M,0}^{N} + W_{M-1,0}^{N}\right) + \frac{1}{2\Delta\theta^2}\left[-\frac{1}{M} W''^{N}_{M,0}\ddot{W}^{N}_{M,0} + \frac{1}{2}\left(M - \frac{1}{2}\right)\left(\dot{W}'\right)^2_{M-1/2,\,1/2}{}^{N-1/2}\right]$$

$$f_{1,n} = -\psi_{M-1,n}\left(W_{M,n} - W_{M-1,n}\right) - \psi_{M,n}\left(3W_{M,n} + W_{M-1,n}\right)$$

$$- \frac{1}{M\Delta\theta^2}\left\{\frac{M}{M-1}\psi_{M-1,n}\ddot{W}_{M-1,n} + \psi_{M,n-1} W''_{M,n-1} - \psi_{M,n}\left(3\ddot{W}_{M,n} + 2W''_{M,n}\right)\right.$$

$$\left. + \psi_{M,n+1} W''_{M,n+1} - 2\left(M - \frac{1}{2}\right)\left[\left(\psi\dot{W}'\right)_{M-1/2,\,n-1/2} - \left(\psi\dot{W}'\right)_{M-1/2,\,n+1/2}\right]\right\}$$

$$f_{2,n} = \frac{1}{2} W''_{M,n}\left(W_{M,n} + W_{M-1,n}\right) + \frac{1}{\Delta\theta^2}\left\{-\frac{1}{M} W''_{M,n}\ddot{W}_{M,n} + \frac{1}{4}\left(M - \frac{1}{2}\right)\left[\left(\dot{W}'\right)^2_{M-1/2,\,n-1/2} + \left(\dot{W}'\right)^2_{M-1/2,\,n+1/2}\right]\right\}$$

Sub-matrices of the Dynamic Matrices A_D and F_D

A_D is a diagonal matrix with entries on the odd numbered row only. It is partitioned into sub-matrices $C_{D,0}(2 \times 2)$, $C_{D,m}(\overline{N} \times \overline{N})$, $(m = 1, 2. \ . \ . M)$. The elements follow:

$$C_{D,0,1,1} = \frac{N\Delta x^4}{4\Delta\tau^2}$$

$$\left.\begin{aligned} C_{D,m,2n+1,2n+1} &= \frac{2m\Delta x^4}{\Delta\tau^2} \qquad n = 1, 2, \ . \ . \ . \ . N-1 \\ C_{D,m,1,1} &= \frac{m\Delta x^4}{\Delta\tau^2} \\ {\scriptstyle 2N-1,2N-1} & \end{aligned}\right\} m = 1, 2, \ . \ . \ . \ . M$$

F_D is a column matrix partitioned into sub-matrices $F_{D,0}(1 \times 2)$, $F_{D,m}$ $(1 \times \overline{N})$, $(m = 1, 2, \ . \ . \ . \ M)$. For $k = 2$ the elements follow.

$$F_{D,0} = \left\{ \begin{matrix} \frac{N\Delta x^4}{2\Delta\tau^2} W_0 \\ 0 \end{matrix} \right\}_{k=1}$$

$$F_{D,m} = \frac{2m\Delta x^4}{\Delta\tau^2} \left\{ \begin{matrix} W_{m,0} \\ 0 \\ \uparrow \\ 2W_{m,n} \\ 0 \\ \downarrow \\ W_{m,N} \\ 0 \end{matrix} \right\}_{k=1} \qquad m = 1, 2, \ . \ . \ . M$$

For $k \geq 3$

$$F_{D,0} = \frac{N\Delta x^4}{8\Delta\tau^2} \begin{cases} 5W_{0,k-1} - 4W_{0,k-2} + W_{0,k-3} \\ 0 \end{cases}$$

$$F_{D,m} = \frac{m\Delta x}{\Delta\tau^2} \begin{cases} \frac{1}{2}\left(5W_{m,0,k-1} - 4W_{m,0,k-2} + W_{m,0,k-3}\right) \\ 0 \\ 5W_{m,n,k-1} - 4W_{m,n,k-2} + W_{m,n,k-3} \\ 0 \\ \frac{1}{2}\left(5W_{mi,N,k-1} - 4W_{m,N,k-2} + W_{m,N,k-3}\right) \\ 0 \end{cases}$$

REFERENCES

1. Huang, N. C., "Axisymmetric Dynamic Snap-through of Elastic Clamped Shallow Spherical Shells," University of California, San Diego, TR-7, February, 1968.

2. Marguerre, K., "Zur Theorie der gekrümmten Platte grosser Formänderung," Proceedings of the Fifth International Congress of Applied Mechanics, 1938.

3. Timoshenko, S. P., and J. M. Gere, Theory of Elastic Stability, McGraw-Hill Book Company, Inc., New York, 1961 (Chapter 11).

4. Thurston, G. A., "Newton's Method Applied to Problems in Nonlinear Mechanics," J. Appl. Mech., 383-388, (1965).

5. Stein, M., and Sanders, J. L., Jr., "A Method for Deflection Analysis of Thin Low-Aspect-Ratio Wings," NACA TN-3640, 1956.

6. Engeli, M., T. Ginsburg, H. Rutishauser, E. Stiefel, "Refined Iterative Methods for Computation of the Solution and the Eigenvalues of Self-Adjoint Boundary Value Problems," Mitteilung aus dem Institut für angewandte Mathematik, Birkhäuser Verlag, Basel/Stuttgart, 1959.

7. Schaeffer, H. G., "The Direct Determination of Nonlinear Displacements of Arbitrarily Supported Shallow Shells using Mathematical Programming Techniques," Ph. D. Thesis, Virginia Polytechnic Institute, Va., April 1967.

8. Houbolt, J. C., "A Recurrence Matrix Solution for the Dynamic Response of Elastic Aircraft," J. Aero. Sci., Vol. 17, 540-550, (1950).

9. Johnson, D. E., "A Proof of the Stability of the Houbolt Method," AIAA J., 4(8), 1450-1451, (1966).

10. Potters, M. L., "A Matrix Method for the Solution of a Second Order Difference Equation in Two Variables," Math. Centrum Report MR19, (1955).

11. Schaeffer, H. G., "Computer Program for Finite-Difference Solutions of Shells of Revolution Under Asymmetric Loads," NASA TN D-3926, (1967).

12. Budiansky, B., and Radkowski, P. P., "Numerical Analysis of Unsymmetrical Bending of Shells of Revolution," AIAA J., 1(8), 1833-1842, (1963).

13. Weinitschke, H., "On the Stability Problem for Shallow Spherical Shells," J. Math. and Phys., Vol. 38, 209-231, (1960).

14. Weinitschke, H. J., "On Asymmetric Buckling of Shallow Spherical Shells," J. Math. and Phys., Vol. 44, 141-163, (1965).

15. Budiansky, B., and Roth, R.S., "Axisymmetric Dynamic Buckling of Clamped Shallow Spherical Shells," NASA TN D-1510, 597-606, (1962).

16. Stephens, W.B., and Fulton, R.E., "Axisymmetric Static and Dynamic Buckling of Spherical Caps Due to Localized Pressures," to be presented at the AIAA, 7th Aerospace Sciences Meeting, New York, January 20-22, 1969.

17. Huang, N.C., "Unsymmetrical Buckling of Thin Shallow Spherical Shells," J. Appl. Mech., 447-457, (1964).

18. Budiansky, B., "Buckling of Clamped Shallow Spherical Shells," Proceedings of the I.U.T.A.M. Symposium of the Theory of Thin Elastic Shells," North Holland Publishing Company, Amsterdam, 64-69, (1960).

19. Ball, R.E., "A Geometrically Nonlinear Analysis of Arbitrarily Loaded Shells of Revolution," NASA CR-909, 1968.

20. Budiansky, B., "Dynamic Buckling of Elastic Structures: Criteria and Estimates," Dynamic Stability of Structures, Pergamon Press, New York, 1966.

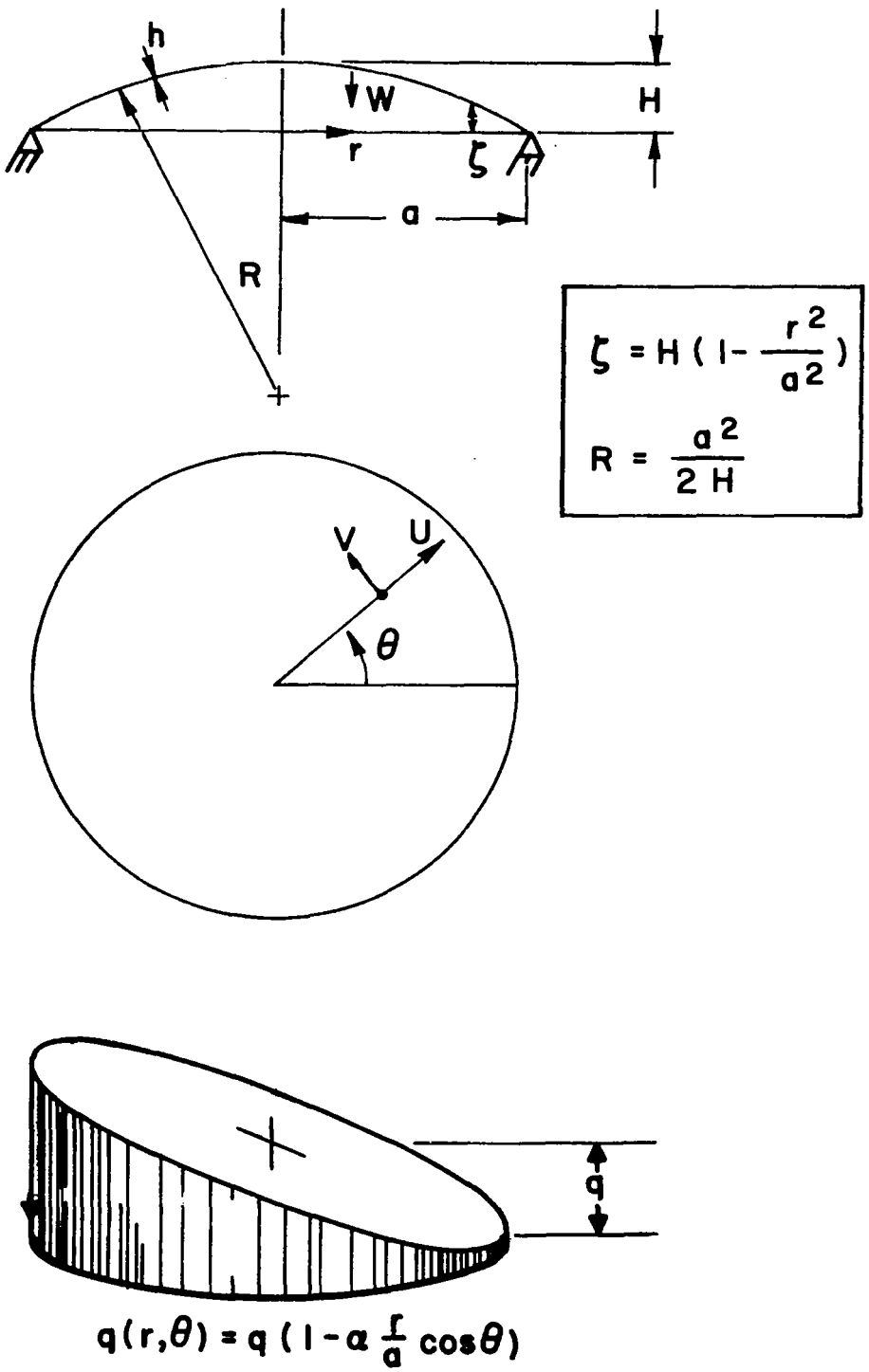

FIG. 1: GEOMETRY, NOTATION, AND LOAD DISTRIBUTION

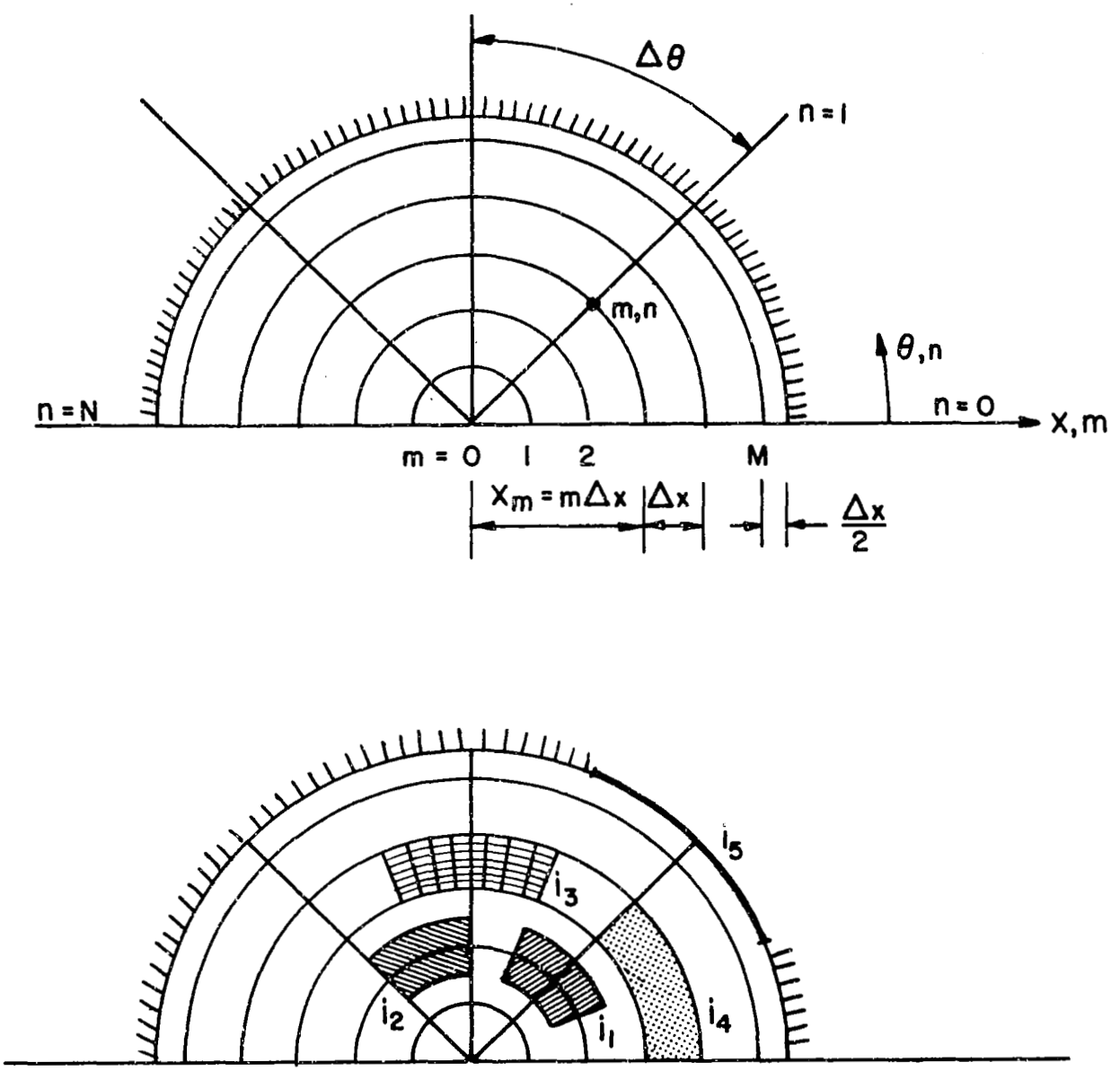

(THE i's ARE DEFINED BY EQUATIONS 19)

FIG. 2: FINITE DIFFERENCE NET, ELEMENTAL AREAS AND LENGTH

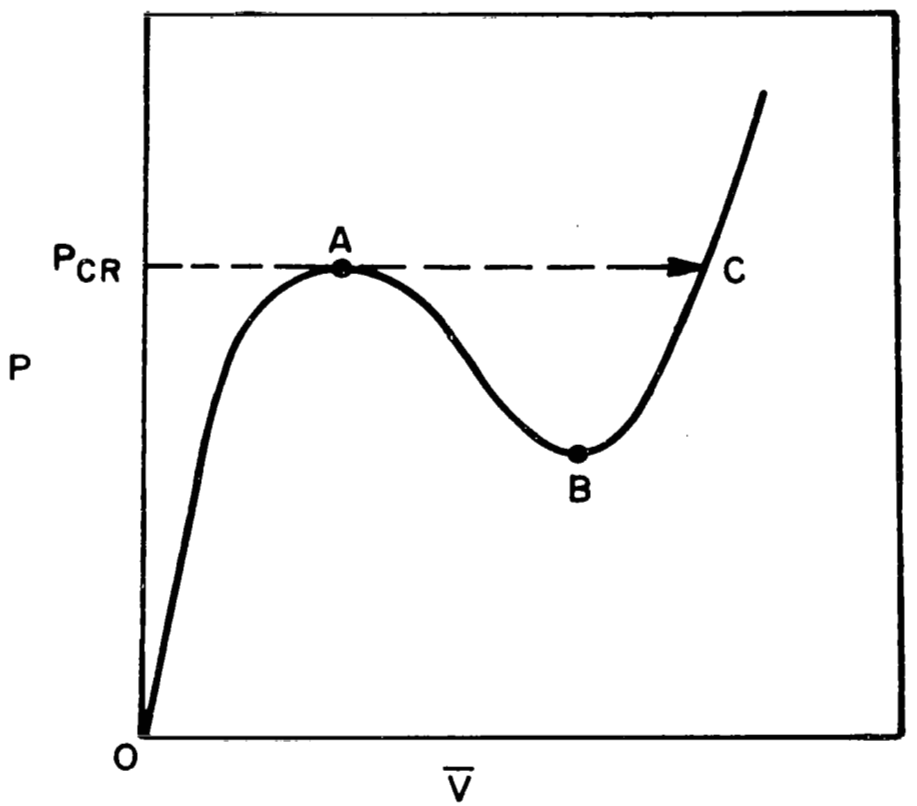

FIG. 3: STATIC LOAD-DEFLECTION CURVE OF SIMPLY SUPPORTED SHALLOW SPHERICAL SHELLS

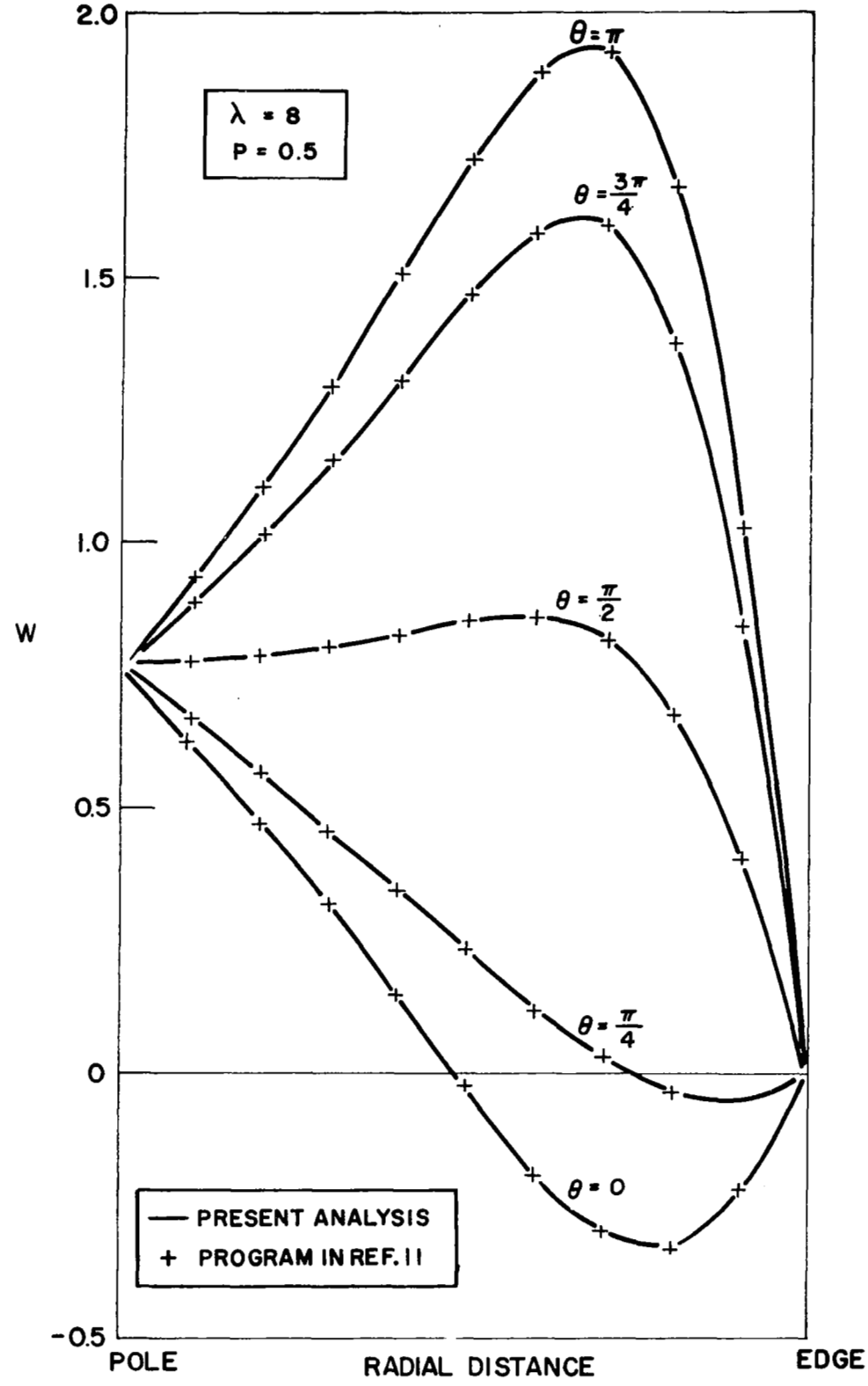

FIG. 4: ASYMMETRIC LINEAR STATIC DEFLECTION

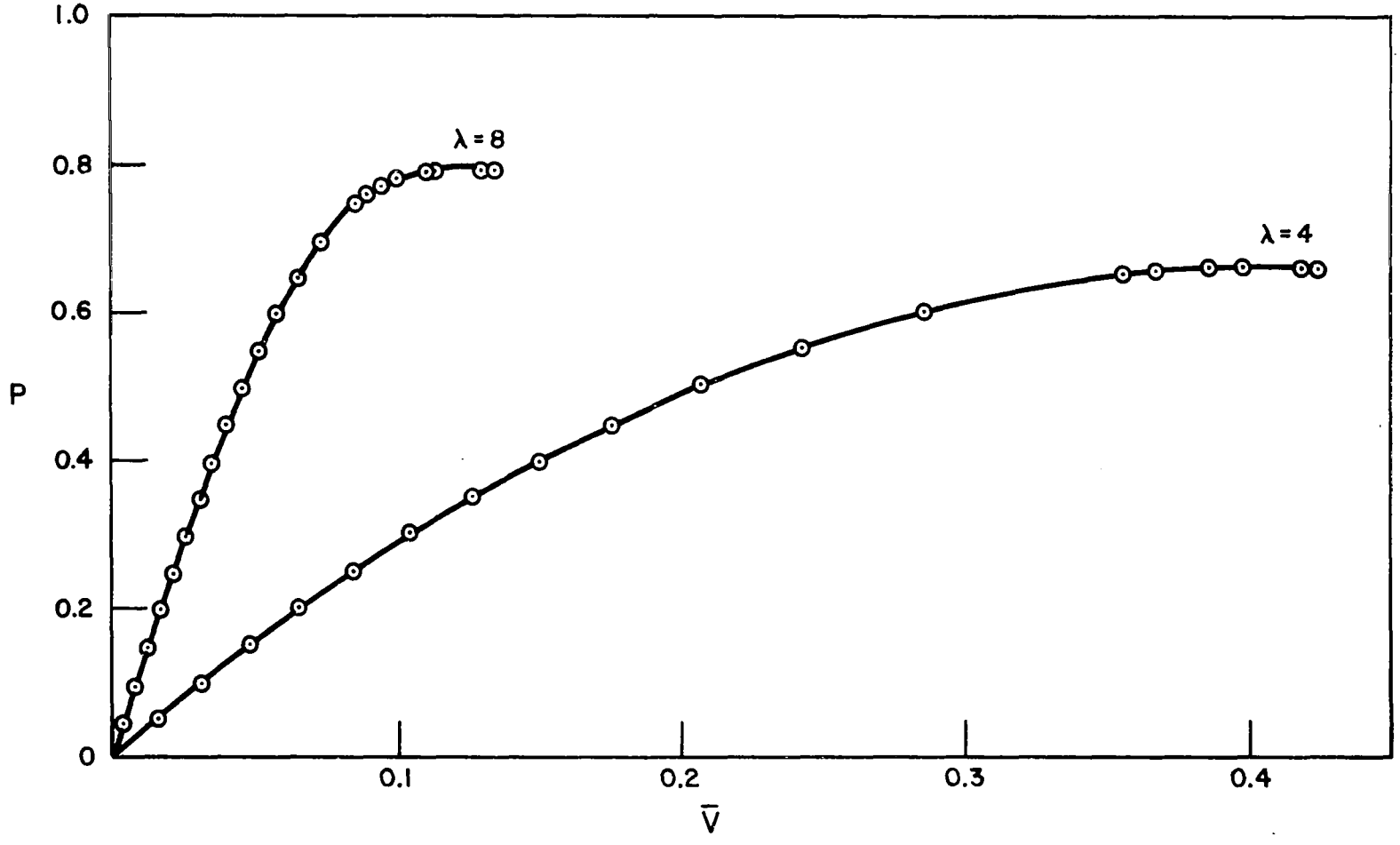

FIG. 5: STATIC LOAD - DEFLECTION CURVES OF UNIFORMLY LOADED SHELLS

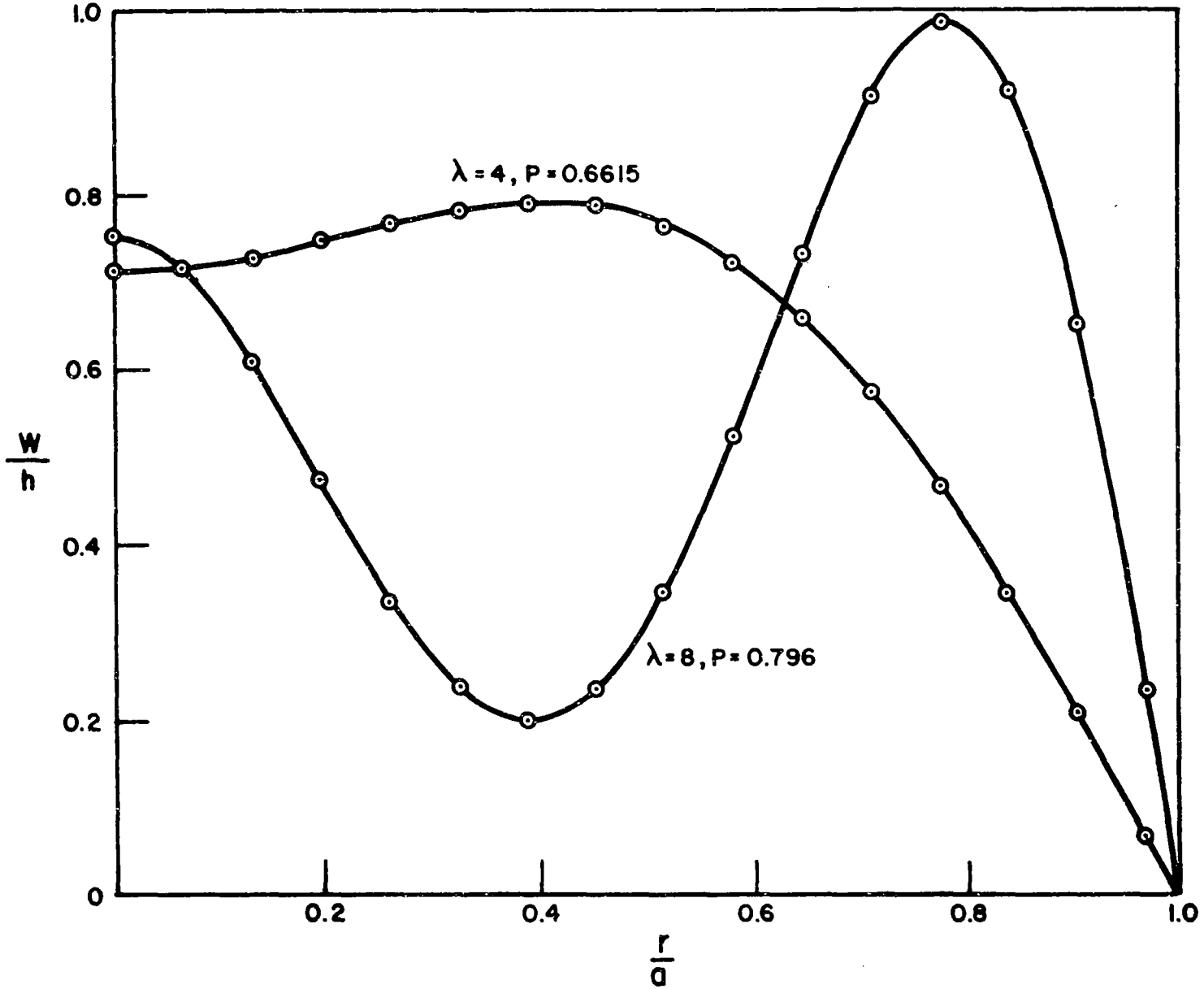

FIG.6: STATIC DEFLECTIONS OF UNIFORMLY LOADED SHELLS

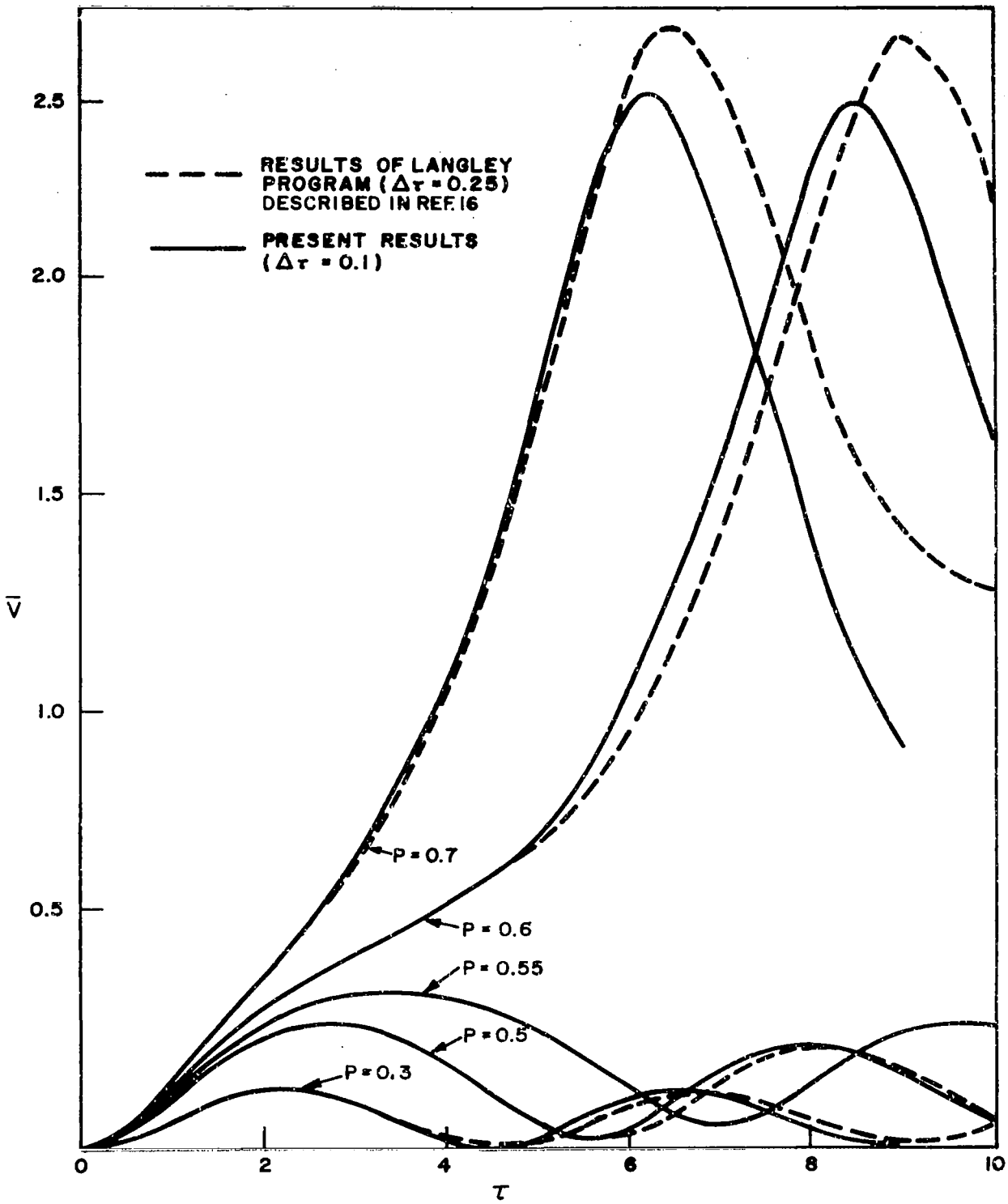

FIG. 7: RESPONSE HISTORIES FOR UNIFORM PRESSURE, $\lambda = 5$

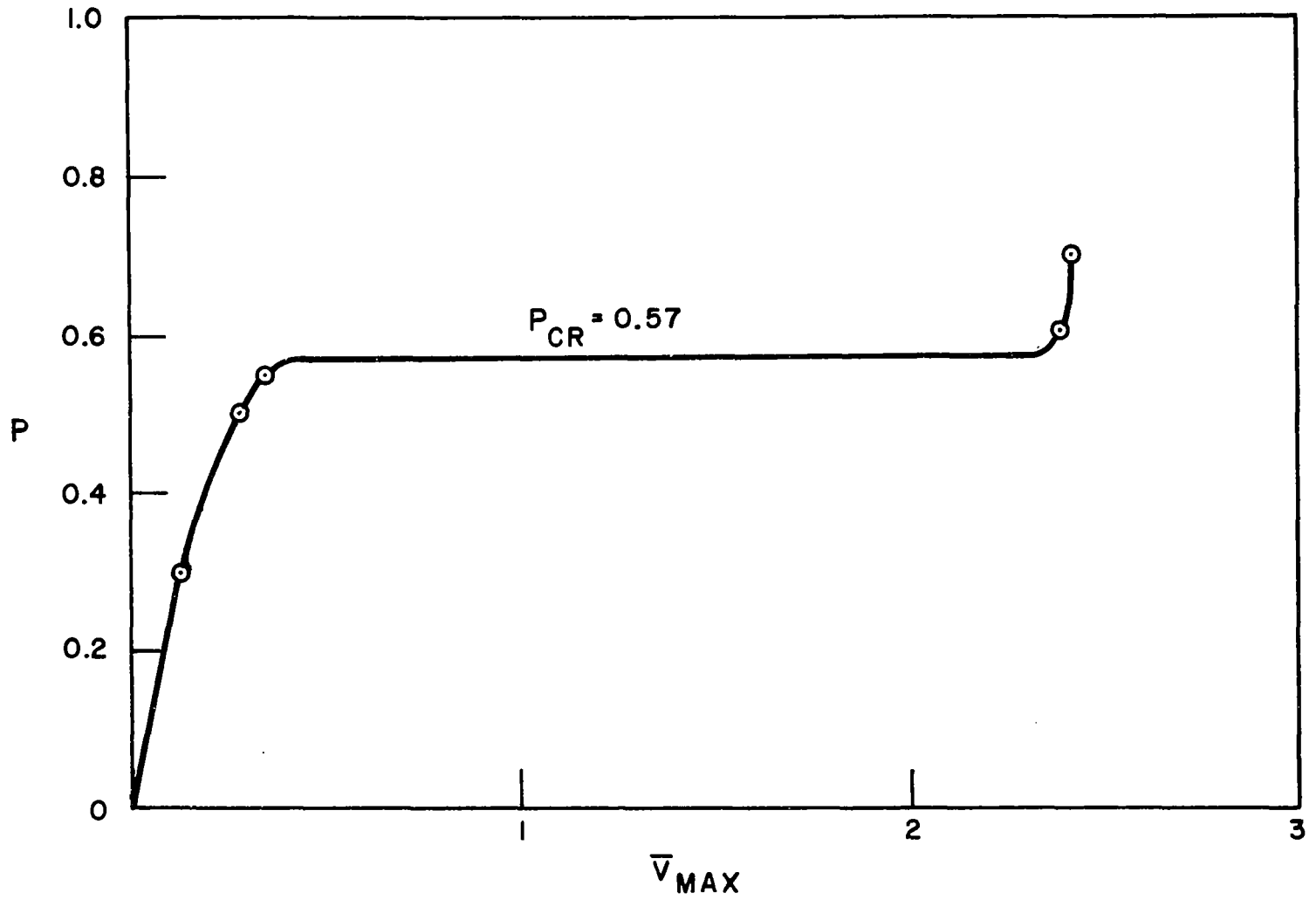

FIG. 8: DYNAMIC LOAD-DEFLECTION CURVE, UNIFORM PRESSURE, $\lambda=5$

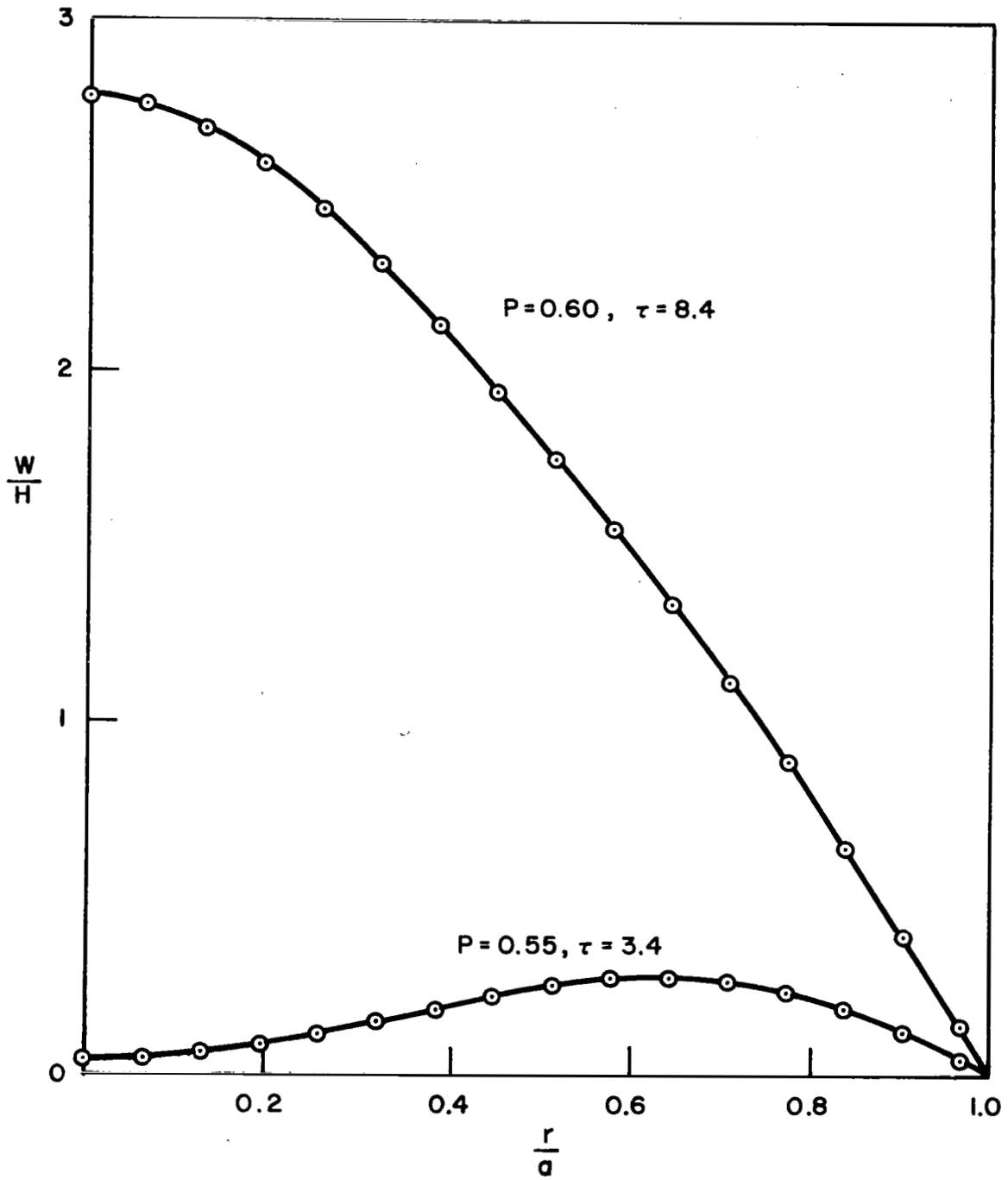

FIG. 9: DEFLECTED SHAPES AT SUB-CRITICAL AND SUPER-CRITICAL LOAD INTENSITIES UNIFORM PRESSURE, $\lambda = 5$

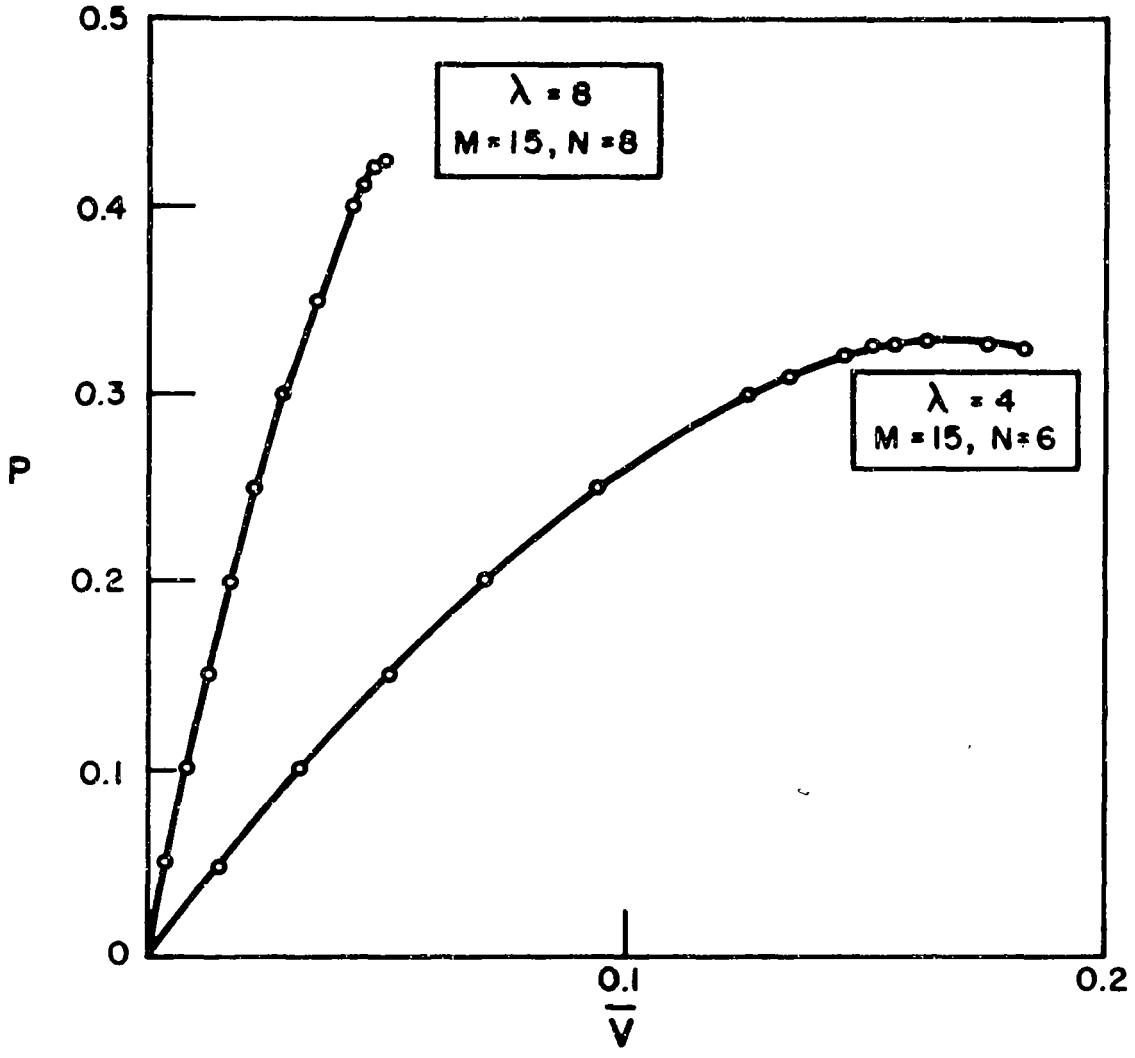

FIG. 10: STATIC LOAD-DEFLECTION CURVES FOR ASYMMETRICALLY LOADED SHELLS

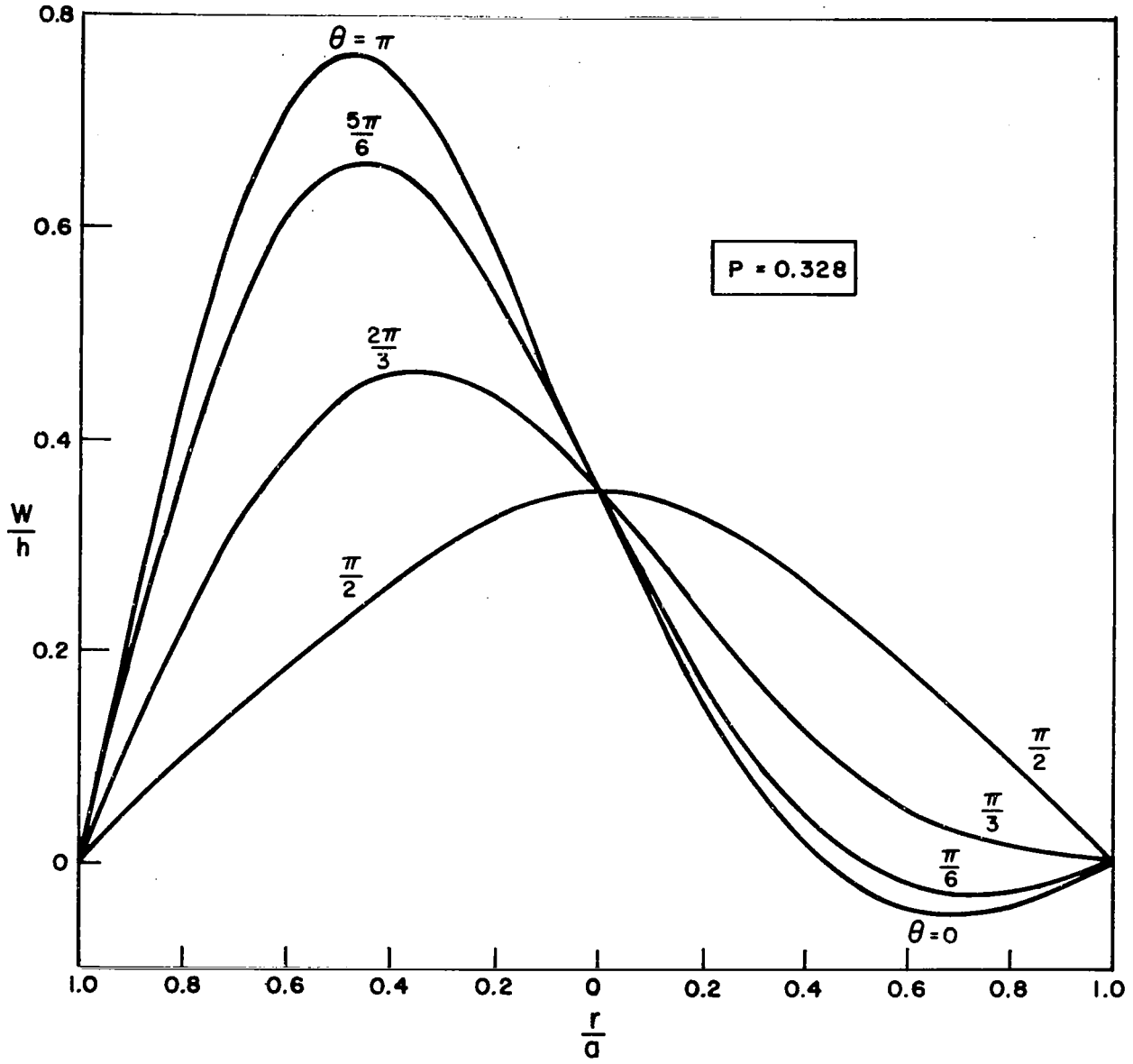

FIG. 11: STATIC DEFLECTION OF ASYMMETRICALLY LOADED SHELL, $\lambda=4$

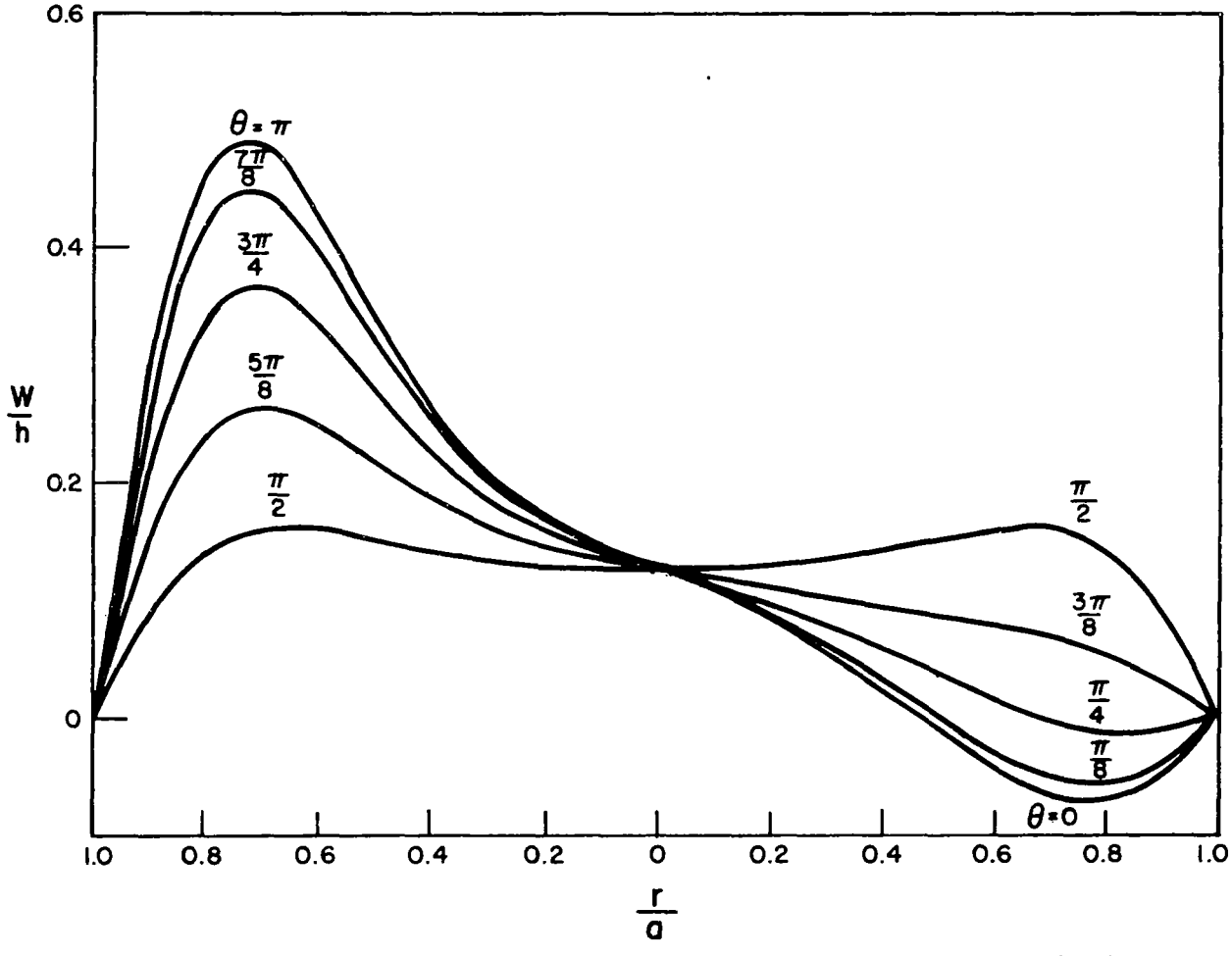

FIG. 12: STATIC DEFLECTION OF ASYMMETRICALLY LOADED SHELL, $\lambda = 8$, $P = 0.300$

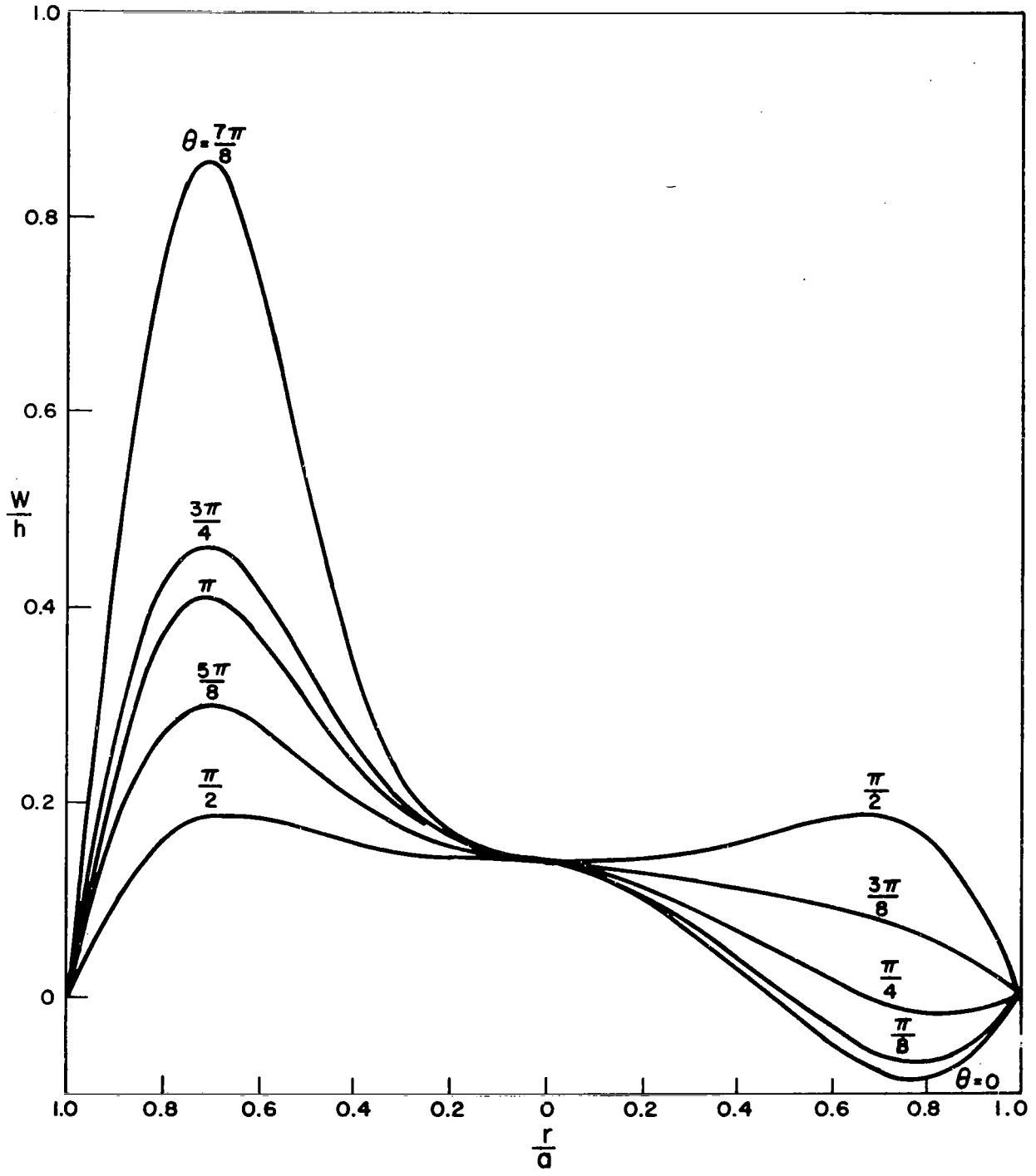

FIG. 13: STATIC DEFLECTION OF ASYMMETRICALLY LOADED SHELL, $\lambda = 8$, $P = 0.350$

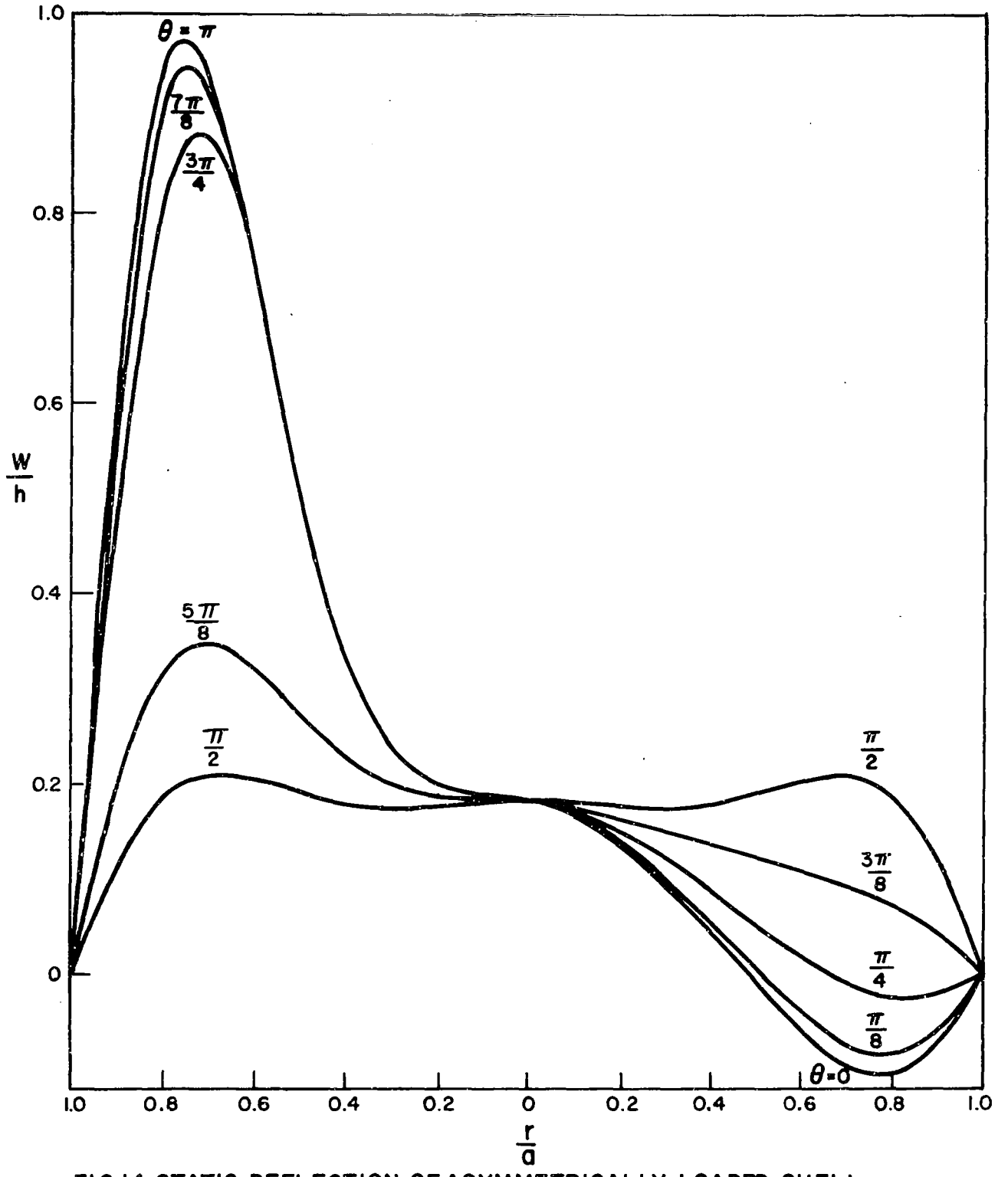

FIG. 14: STATIC DEFLECTION OF ASYMMETRICALLY LOADED SHELL, $\lambda = 8$, $P = 0.425$

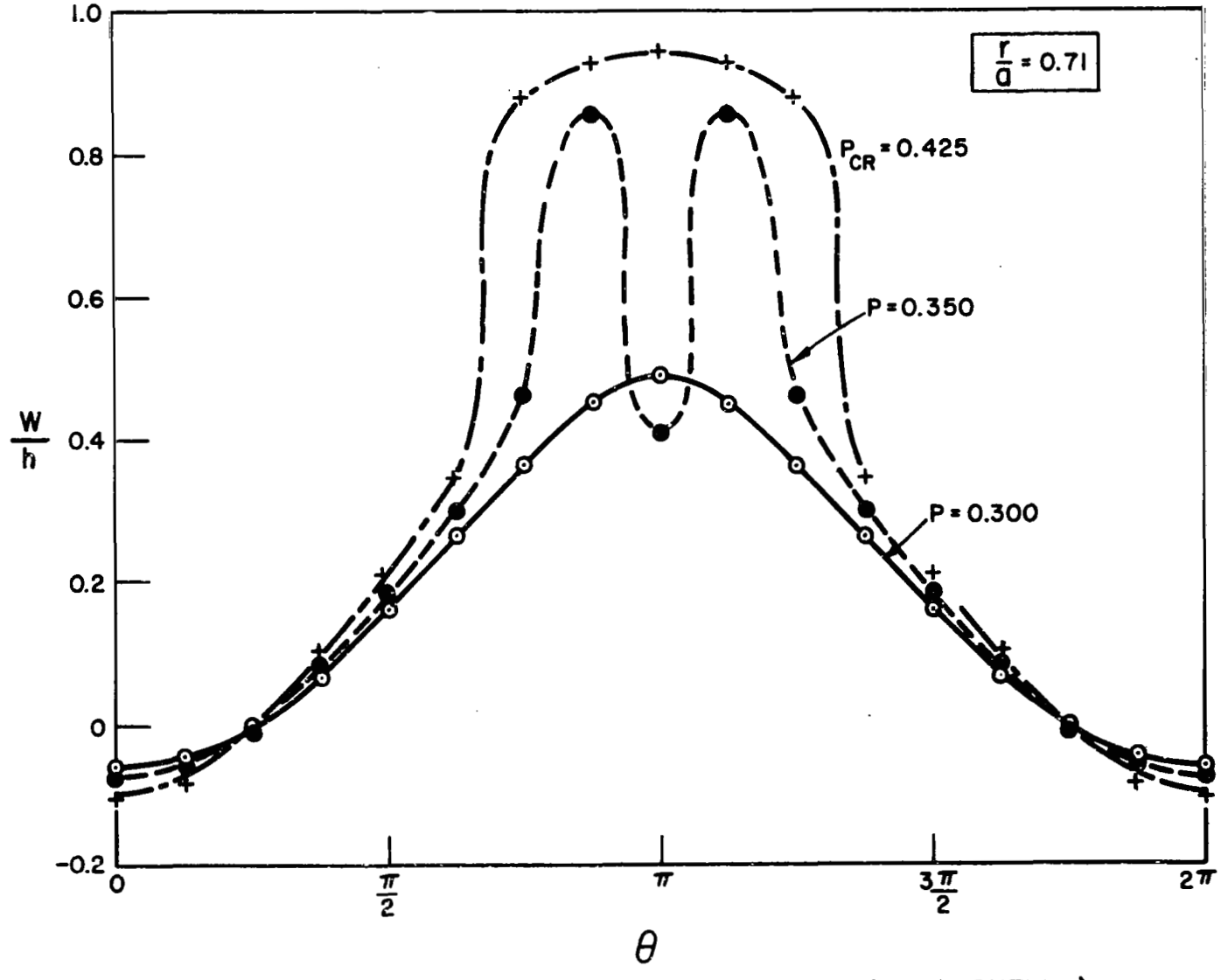

FIG. 15: STATIC DEFLECTION OF ASYMMETRICALLY LOADED SHELL, $\lambda = 8$, AT VARIOUS LOAD LEVELS

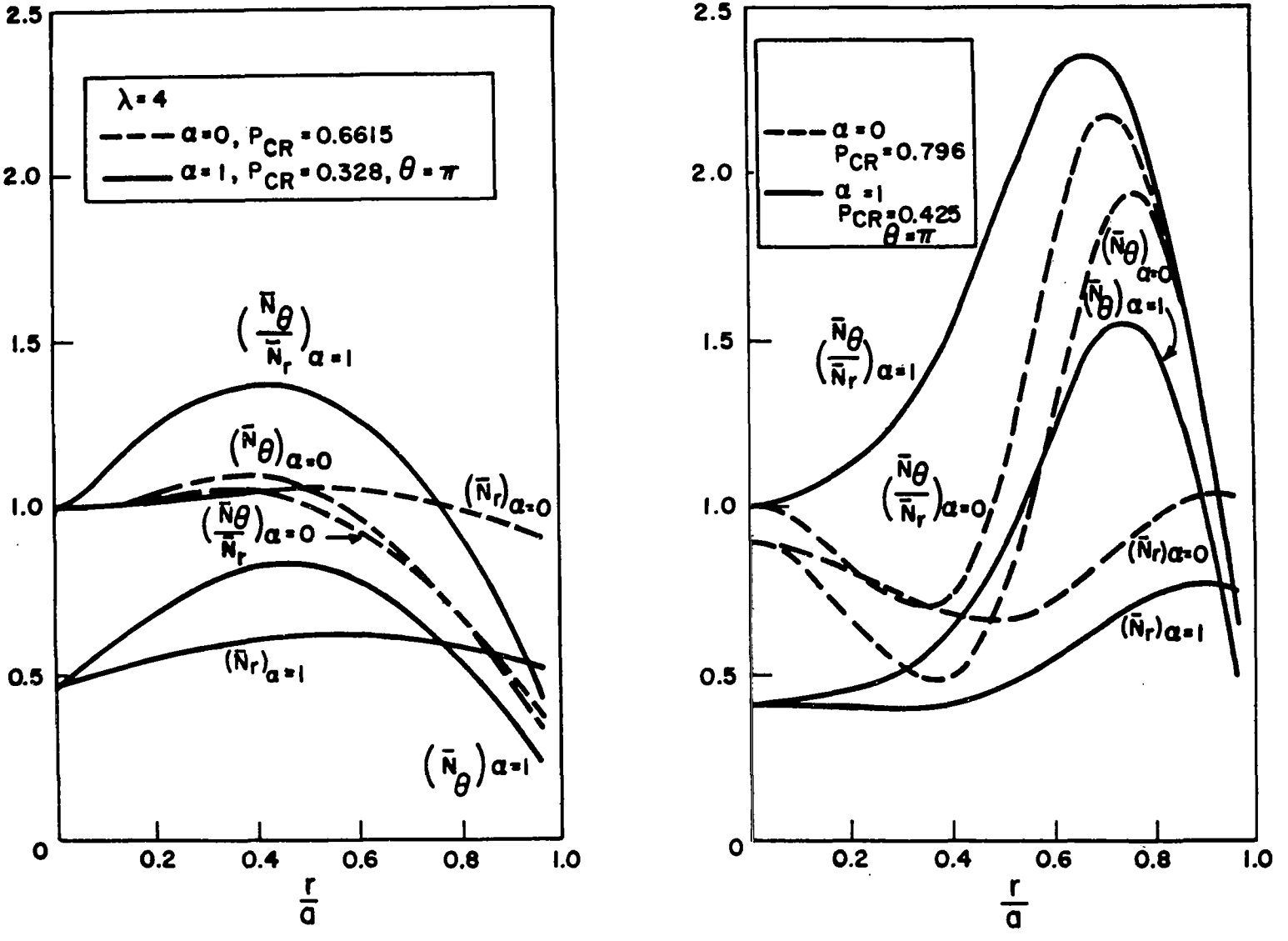

FIG. 16: STATIC MEMBRANE STRESSES IN AXISYMMETRICALLY AND ASYMMETRICALLY LOADED SHELLS

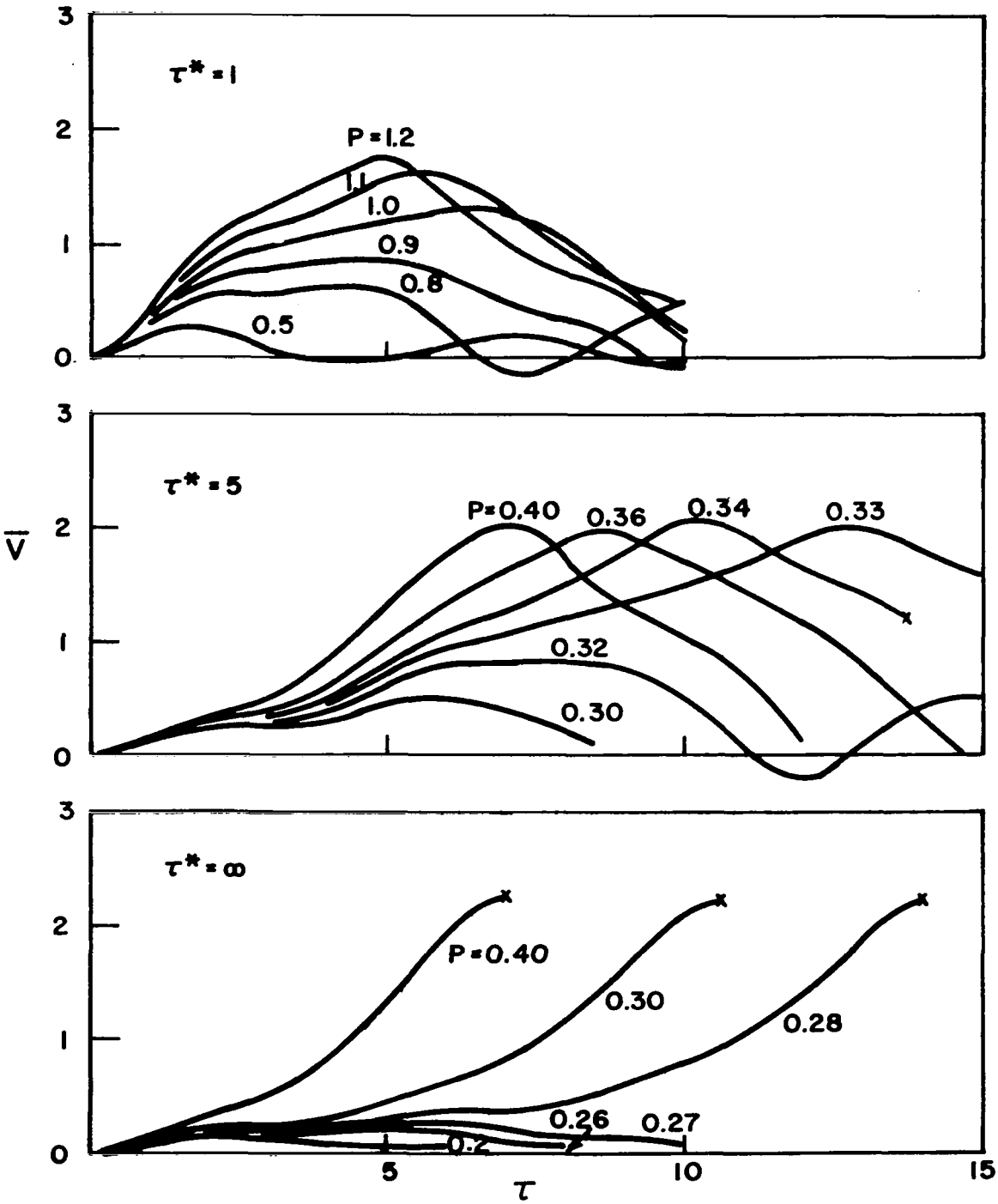

FIG. 17: RESPONSE HISTORIES FOR ASYMMETRICALLY LOADED SHELLS, $\lambda = 4$

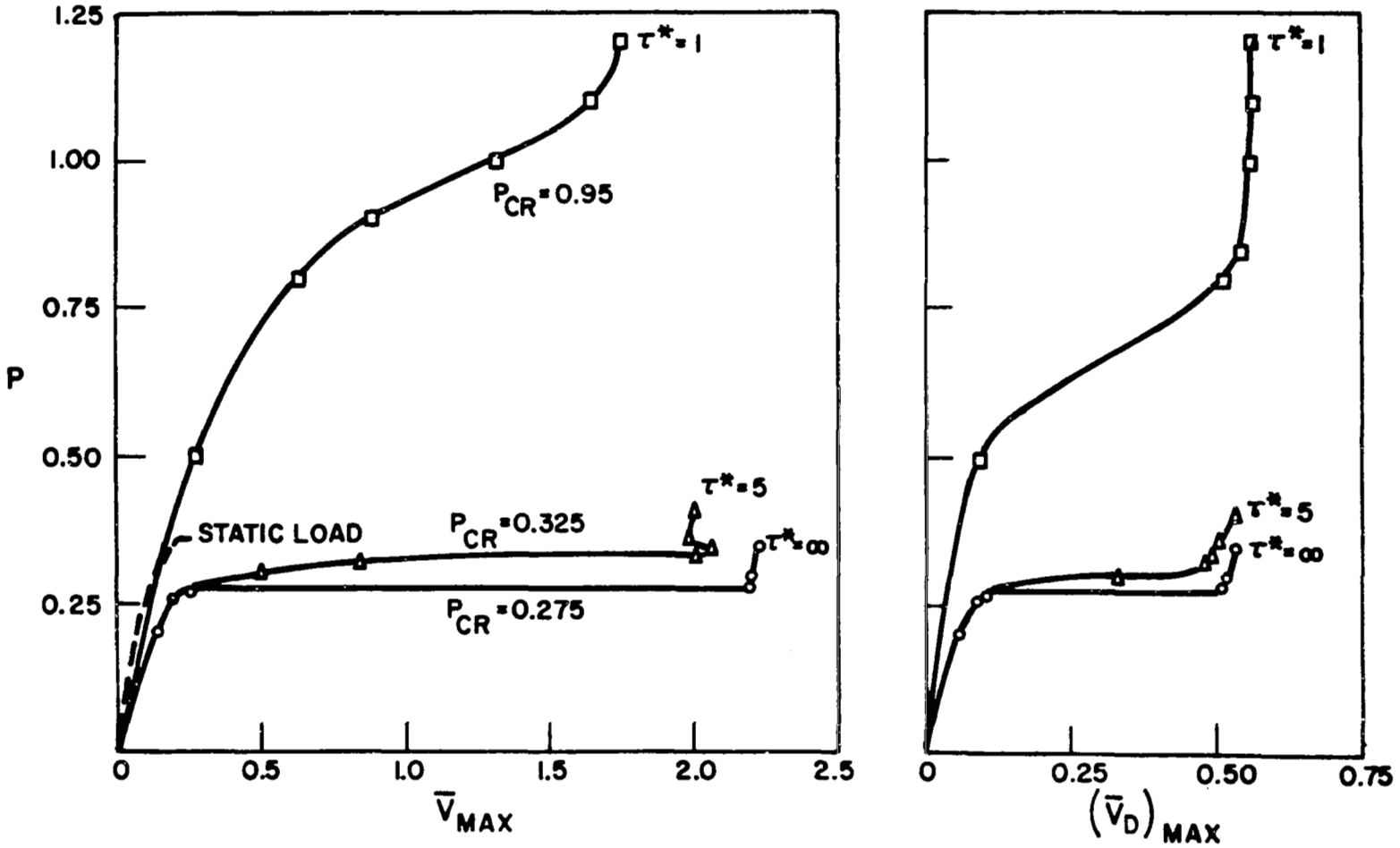

FIG. 18: DYNAMIC LOAD-DEFLECTION CURVES FOR ASYMMETRICALLY LOADED SHELLS, $\lambda = 4$

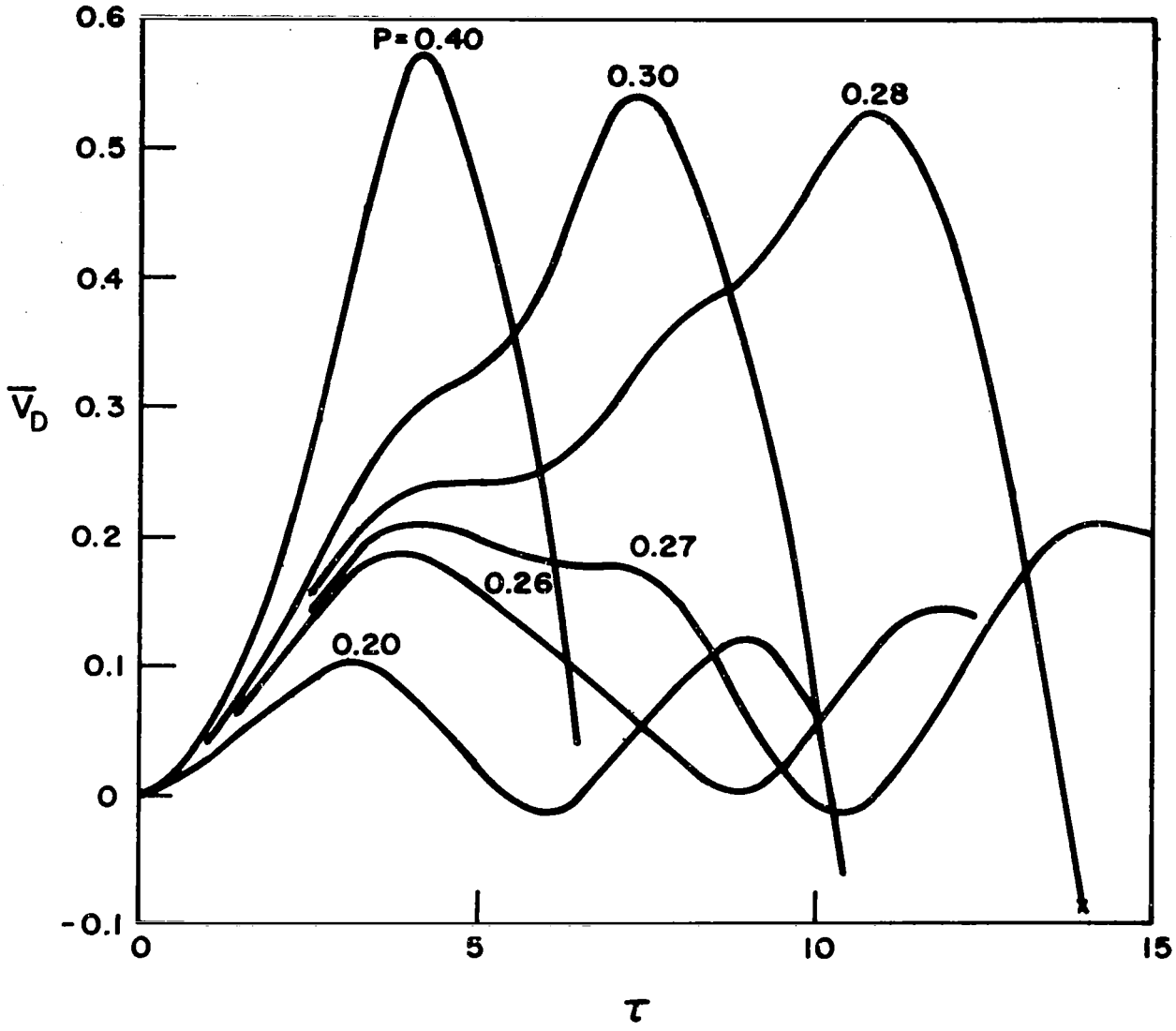

FIG. 19: $\overline{V}_D$ HISTORIES FOR $\lambda = 4$, $\tau^* = \infty$

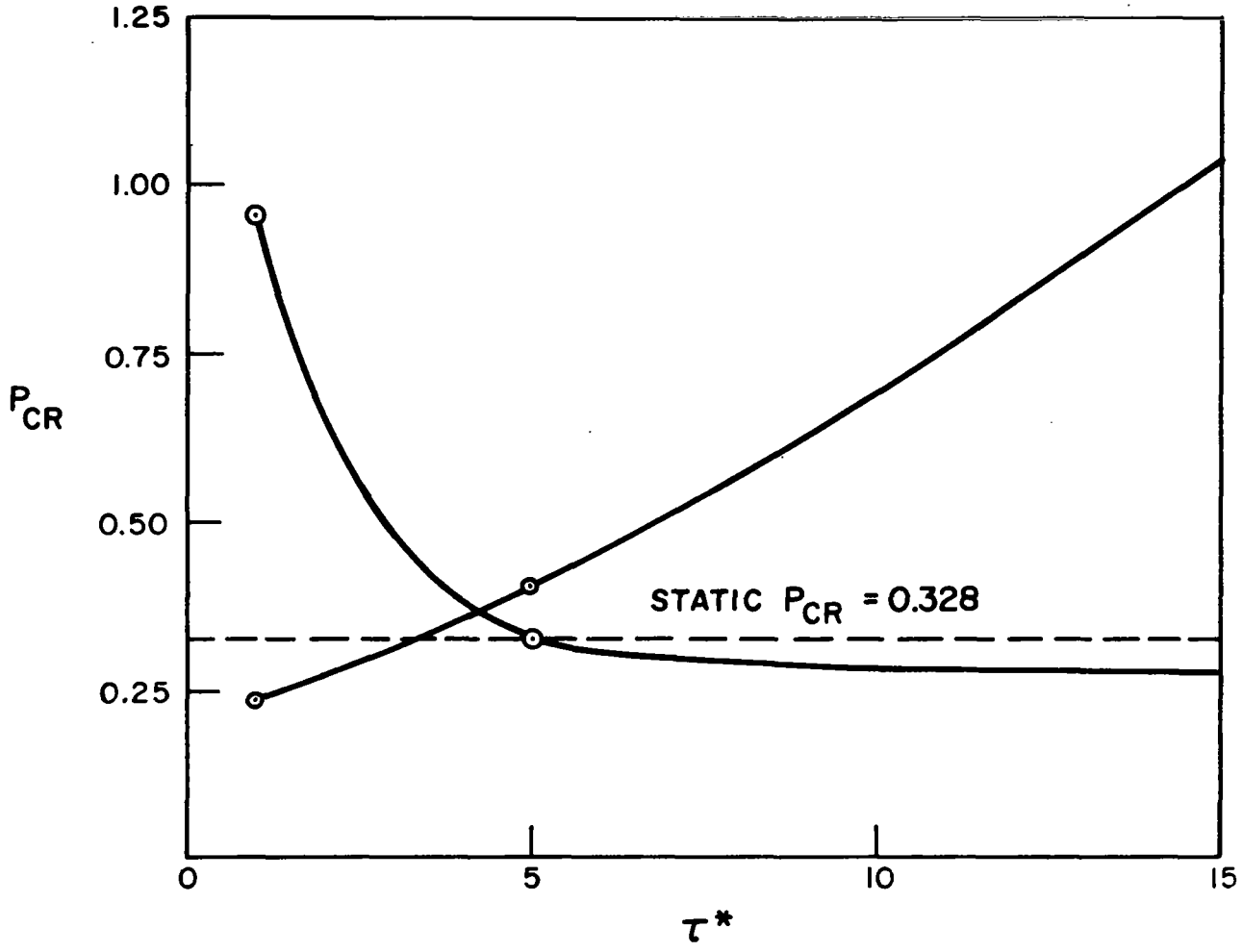

FIG. 20: VARIATION OF P_{CR} AND I_{CR} WITH τ^* FOR ASYMMETRICALLY LOADED SHELLS WITH $\lambda = 4$

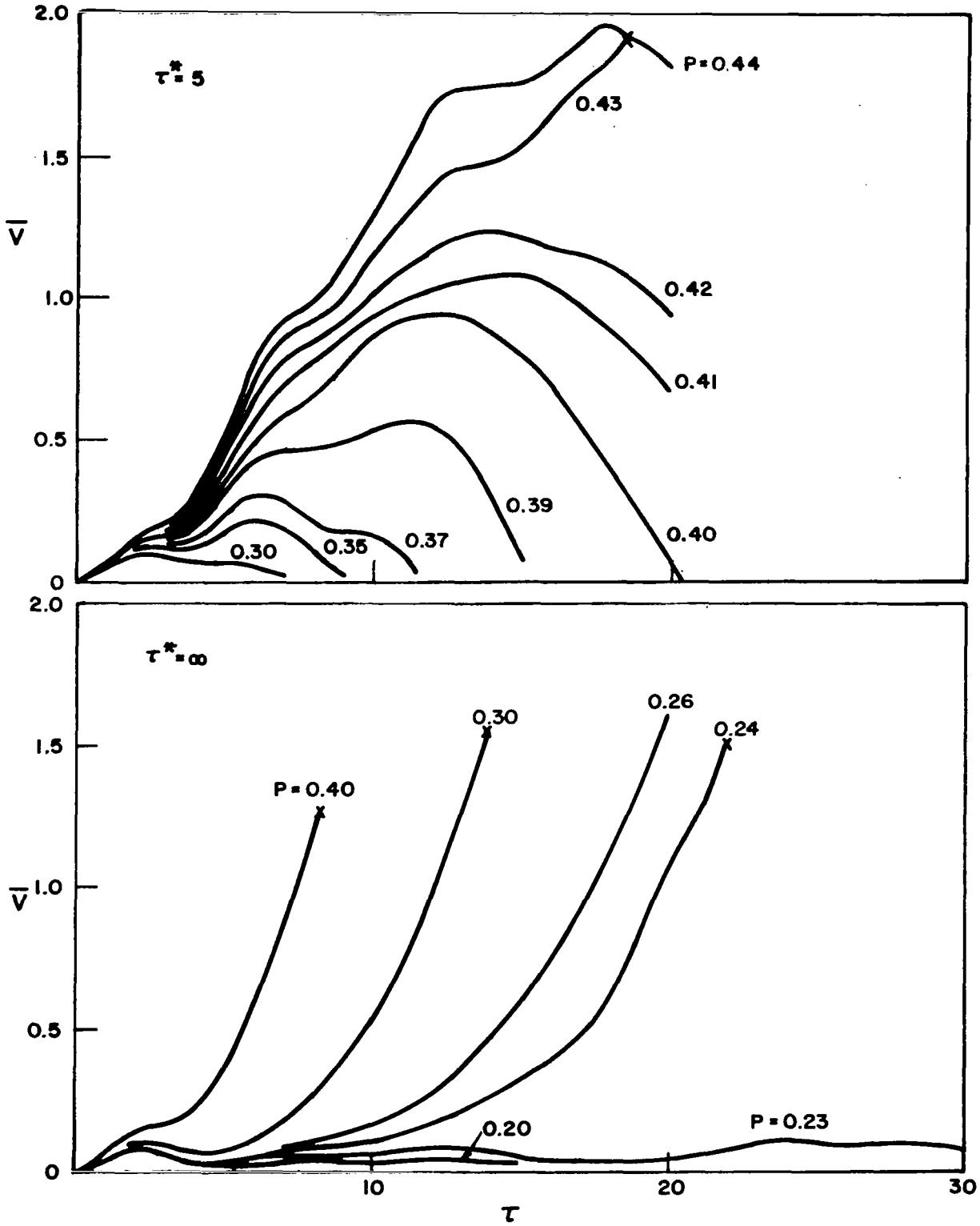

FIG.21: RESPONSE HISTORIES FOR ASYMMETRICALLY LOADED SHELLS, $\lambda = 6$

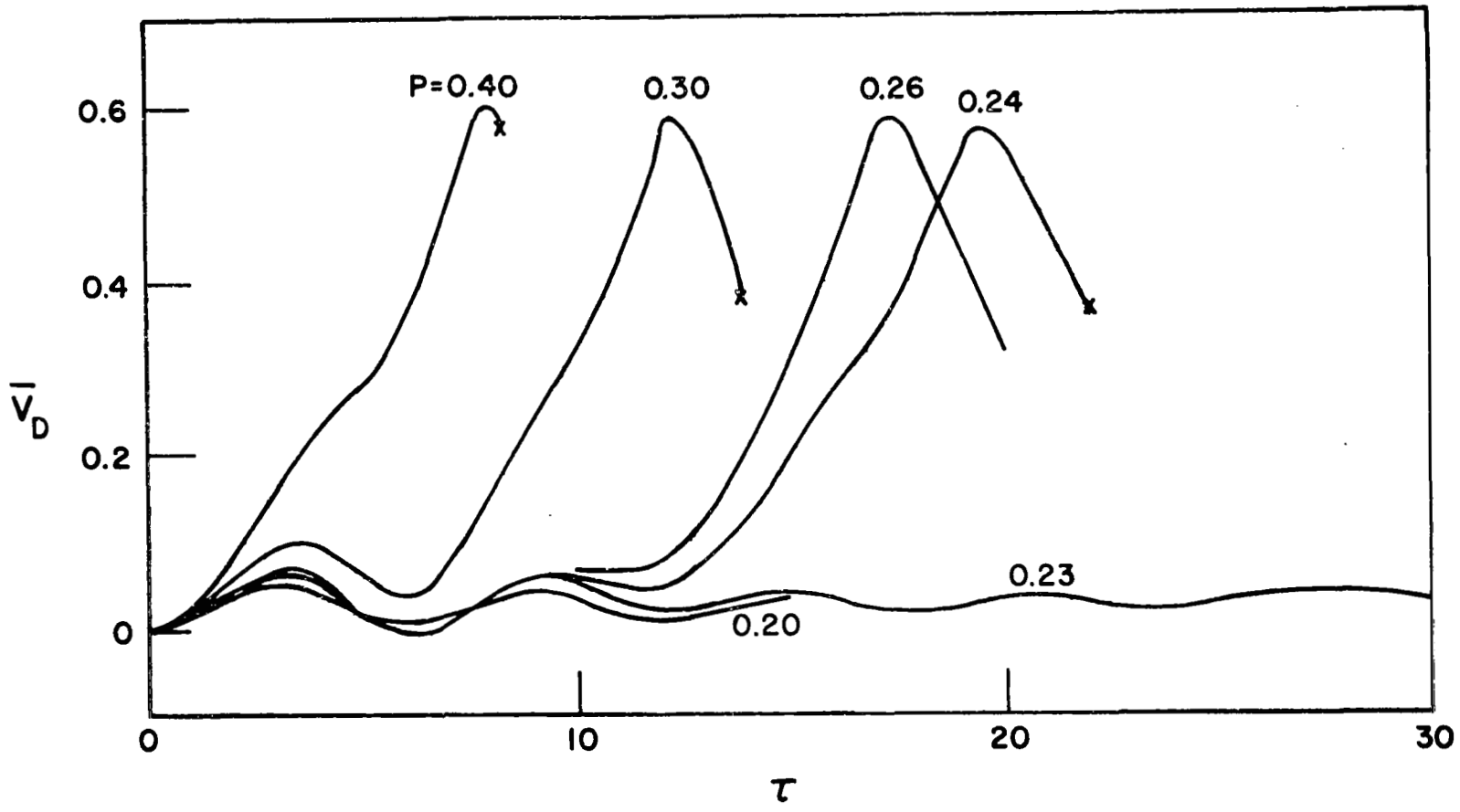

FIG. 22: $\overline{V}_D$ HISTORIES FOR $\lambda = 6$, $\tau^* = \infty$

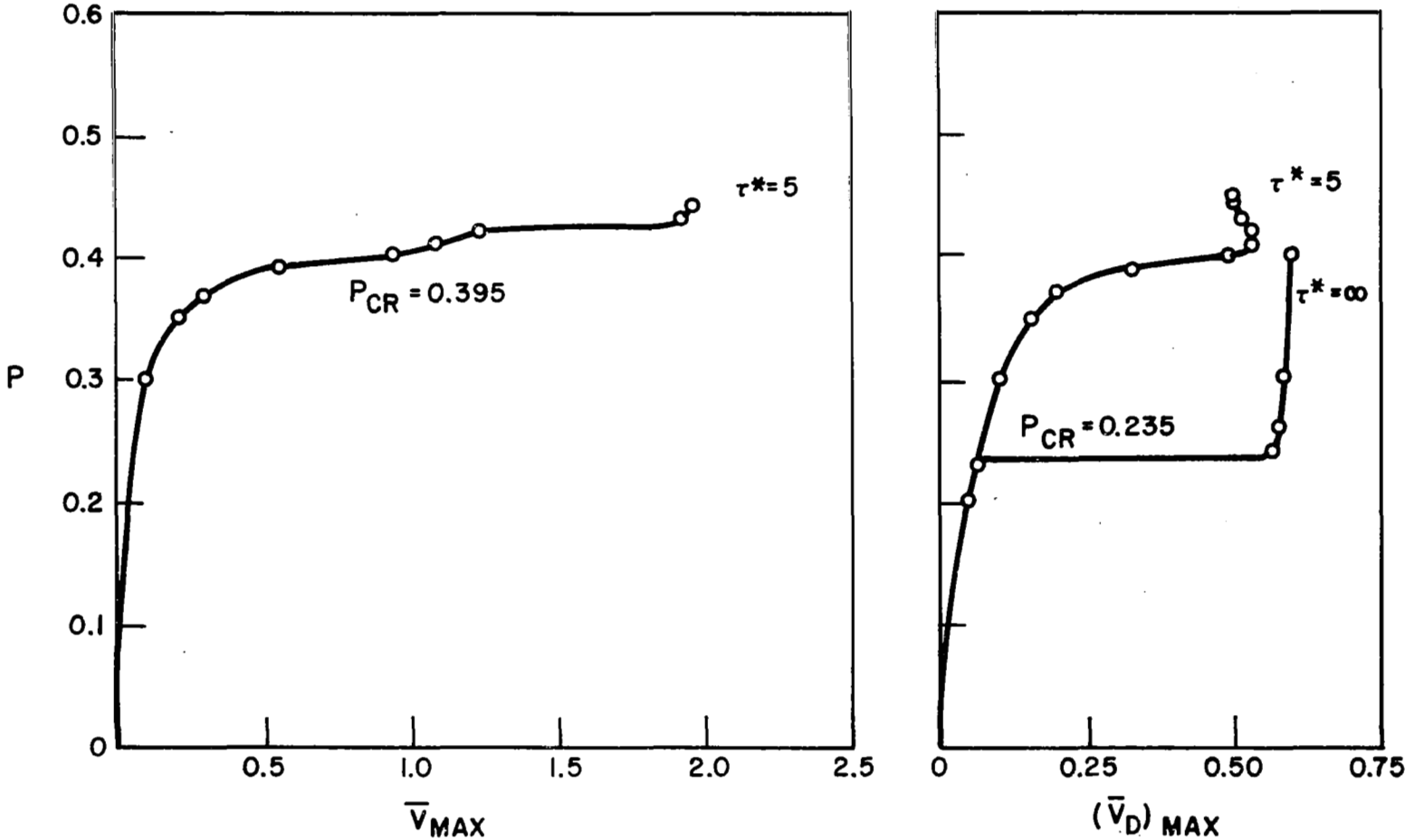

FIG. 23: DYNAMIC LOAD-DEFLECTION CURVES FOR ASYMMETRICALLY LOADED SHELLS, $\lambda = 6$

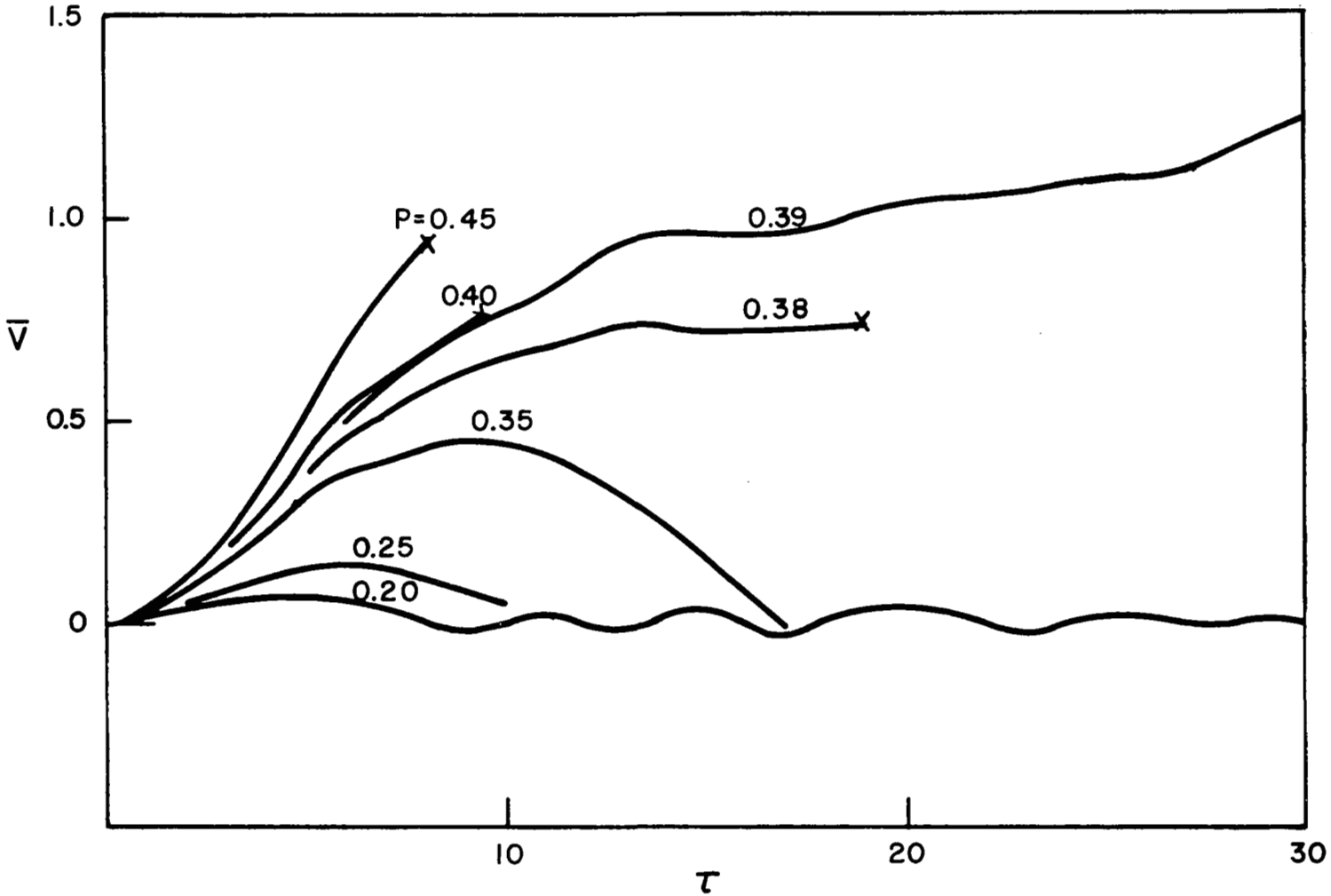

FIG. 24: RESPONSE HISTORIES FOR ASYMMETRICALLY LOADED SHELLS $\lambda=8$

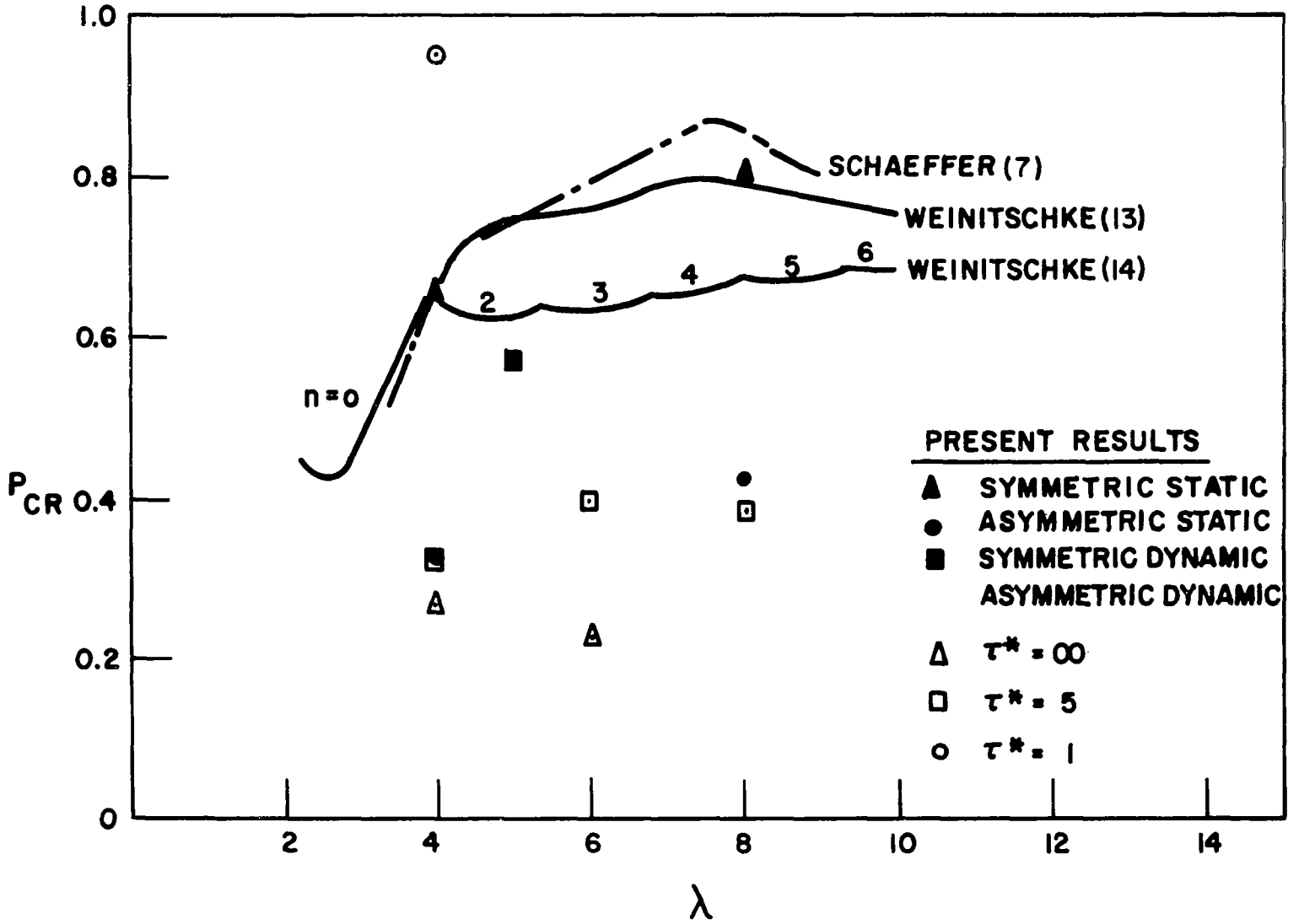

FIG. 25: SUMMARY OF BUCKLING LOADS FOR SIMPLY SUPPORTED SHALLOW SPHERICAL SHELLS